

OCDO--95010716

OHIO COAL RESEARCH CONSORTIUM

SUBCONTRACT AGREEMENT NO. OCRC/93-4.14

OCDO Grant No. CDO/R-87-2C/B

ADSORPTION AND DESORPTION OF SULFUR DIOXIDE ON NOVEL
ADSORBENTS FOR FLUE GAS DESULFURIZATION

Final Report for the Period
September 1, 1993 to August 31, 1994

by

Y.S. Lin
Shuguang Deng

RECEIVED

MAR 20 1995

DEPARTMENT OF DEVELOPMENT
OHIO COAL DEV OFFICE

University of Cincinnati, Cincinnati, OH

February 1995

Project Manager: Y.S. Lin, Associate Professor, Department of Chemical
Engineering, University of Cincinnati, Cincinnati, OH 45221
(513) 556-2769

This project was funded in part by the Ohio Coal Development Office, Department of
Development, State of Ohio.

DISTRIBUTION OF THIS DOCUMENT IS UNLIMITED

MASTER

ct

DISCLAIMER

**Portions of this document may be illegible
in electronic image products. Images are
produced from the best available original
document.**

Table of Contents

Executive Summary	1
Introduction	5
Technical Discussion	9
1. Adsorbent Synthesis and Characterization	9
2. Stability Tests of FGD Adsorbents	14
3. Adsorption and Desorption of SO ₂ in Zeolite Adsorbents	18
4. Sulphation and Regeneration on Alumina Supported FGD Adsorbents	21
Marketing/Commercialization Discussion	23
1. Commercialization of Adsorbent Production	23
2. Recovery of SO ₂ from FGD Process	24
3. Future Work Plans	25
Literature Cited	27
Appendices	33
1. Experimental Set-up	33
2. Figures in This Report	36
3. Tables in This Report	52

Executive Summary

Dry regenerative sorption processes have recently attracted increasing attention in flue gas desulfurization (FGD) because of their several advantages over the conventional wet-scrubbing processes. Dry sorbents are usually made by coating a transition or alkaline earth metal precursor on the surface of a porous support. Major disadvantages of these sorbents prepared by the conventional methods include relatively poor attrition resistance and low SO_2 sorption capacity. The physical and especially chemical attrition (associated with the sulphation-oxidation-reduction cycles in the process) deteriorates the performance of the sorbents. The low SO_2 sorption capacity is primarily due to the small surface area of the support. Materials with a high surface area are not used as the supports for FGD sorbents because these materials usually are not thermally stable at high temperatures.

In the past year, the research supported by OCDO was focused on synthesis and properties of sol-gel derived alumina and zeolite sorbents with improved properties for FGD. The sol-gel derived alumina has large surface area, mesopore size and excellent mechanical strength. Some alumina-free zeolites not only posses the basic properties required as a sorbent for FGD (hydrophobicity, thermal and chemical stability, mechanical strength) but also have extremely large surface area and selective surface chemistry. The major objectives of this research program were to synthesize the sol-gel derived sorbents and to explore the use of the zeolites either directly as adsorbents or as sorbent support for FGD. The research was aimed at developing novel FGD sorbents possessing better sorption equilibrium and kinetic properties and improved physical and chemical attrition resistance.

The original objectives of the research proposed for year four were to investigate the SO_2 sorption and desorption, regeneration, properties of a sol-gel derived $\text{CuO}/\gamma\text{-Al}_2\text{O}_3$ sorbent and zeolite silicalite. Improvement on the synthesis conditions of the $\text{CuO}/$

γ -Al₂O₃ sorbent, and study on the thermal and chemical stability of these two sorbents were also included in the research proposed for year four. During the course of the investigation in year four, the research was extended to include sol-gel derived CaO/ γ -Al₂O₃ sorbents and another hydrophobic and thermal stable zeolite (the DAY zeolite). Therefore, the research in year four was specifically aimed at (1) synthesis of CuO/ γ -Al₂O₃ and CaO/ γ -Al₂O₃ sorbents by the sol-gel method; (2) test of the thermal and chemical stability of these sorbents and (3) measurements of SO₂ sorption and desorption (regeneration) equilibrium and kinetics on CuO/ γ -Al₂O₃, CaO/ γ -Al₂O₃, silicalite and the DAY zeolite sorbents.

Two sol-gel methods were developed to synthesize CuO/ γ -Al₂O₃ and CaO/ γ -Al₂O₃ sorbents. In both methods, the support γ -Al₂O₃ was synthesized by hydrolysis and condensation of an aluminum metal oxide. The acceptor was coated to the support by, in the first method, mixing a solution containing precursor of the acceptor into the alumina (boehmite) sol, and, in the second method, wet-impregnating the calcined sol-gel derived γ -Al₂O₃ with a precursor containing solution. The sorbent synthesized have surface area, pore volume and average pore size of about 250 m²/g, 0.4 ml/g and 40 Å, respectively. XRD data suggest that acceptor amounting up to 40 wt% can be coated on the grain surface of the alumina support. The acceptor appears to be present in a form of two dimensional layer on the grain surface of the support.

The sol-gel derived alumina sorbents have a good thermal and chemical stability. The surface area of these sorbents, after treatments under conditions much more harsh than those encountered in practical use of these sorbents, is still larger than that of sorbents commercially used for FGD. As these alumina sorbent particles consist of fine grains of γ -Al₂O₃ strongly bound by necks of the same material formed through sintering, these sol-gel derived sorbents appear to be mechanically very strong. The zeolites studied also exhibit extremely good chemical and thermal stability.

The sol-gel derived $\text{CuO}\gamma\text{-Al}_2\text{O}_3$ can take 5.66 mmol SO_2 per gram of sorbent, larger than the CuO sorbents prepared by other method (1.03 mmol/g). The sol-gel derived $\text{CuO}/\gamma\text{-Al}_2\text{O}_3$ can be completely regenerated using H_2/N_2 . SO_2 sorption and regeneration rates on the sol-gel derived $\text{CuO}/\gamma\text{-Al}_2\text{O}_3$ sorbent are also greater than those on the CuO sorbents prepared by other method. SO_2 sorption and regeneration properties of the sol-gel derived $\text{CaO}/\gamma\text{-Al}_2\text{O}_3$ sorbent are not as good as those of the $\text{CuO}/\gamma\text{-Al}_2\text{O}_3$ sorbent in terms of equilibrium sorption capacity and sorption/regeneration rate.

The adsorption isotherms of SO_2 on the DAY zeolite and silicalite were measured at temperatures ranging from 25 $^{\circ}\text{C}$ to 100 $^{\circ}\text{C}$ and SO_2 partial pressures up to about 40 mmHg (with air, at total pressure of 760 mmHg). All the adsorption isotherms could be well correlated by the Freundlich equation. The heats of adsorption for the DAY zeolite is 6.9 kJ/mole, smaller than of silicate, 16.9 kJ/mole. The DAY zeolite also adsorbs less amount of SO_2 than silicalite under the same conditions. These results indicate that the DAY zeolite has a weaker affinity with SO_2 as compared to silicalite, although the former has a larger surface area and pore size. The adsorption rate constants for the DAY zeolite and silicalite are essentially the same, regardless the substantial difference in the intracrystalline diffusivity of these two zeolites. This suggests that adsorption of SO_2 on the internal surface of the zeolites is the rate-limiting step.

This research project in year four proceeded as anticipated and achieved expected results described in the proposal, although the project was not in place until the end of November, 1993. The work performed in year four was focused on the synthesis and properties of FGD adsorbents with improved properties, not on development of new FGD processes. It is difficult to provide enough and accurate economic information, at this stage, about the FGD process employing the new adsorbents developed in this work. These adsorbents will be used in dry and self-contained sorption process in which SO_2 is recovered as a useful product and no waste is generated. Based on the developed technology, the operating costs of the sorption process employing the sol-gel derived

adsorbents developed in this work are estimated to be less than \$200/ton of sulfur removed.

The research project will continue in year five with support from OCDO. The anticipated steps following the work performed in year four include (1) synthesis of the CuO/DAY zeolite sorbent and the alumina sorbents in pellet form; (2) measurements of SO₂ sorption and regeneration on the CuO/DAY sorbent, and of the mechanical strength and attrition resistance of the CuO/ γ -Al₂O₃, CaO/ γ -Al₂O₃ and zeolite sorbents and (3) experiments on removal of SO₂ from simulated flue gas using the sorbents developed. It is expected that at the end of year five the novel adsorbents with desired properties and in practically applicable form will be available for pilot tests in FGD sorption process.

Introduction

Combustion (flue) gas produced by coal-burning contains numerous air pollutants, such as NO_2 , NO, CO, CO_2 , H_2S and, most notably, SO_2 . The control of SO_2 and NO_x emission has come to be regarded as a matter of great importance by both the governmental regulating agencies and the general public. Numerous techniques have been developed for flue gas desulfurization (FGD). Majority of the FGD processes is based on throwaway wet- (or dry-) scrubbing technique using limestone as absorption reagent because of low capital and operating costs of these techniques [1, 2]. Dry regenerative FGD processes (e.g., fluidized copper oxide process) have received increasing attention [3, 4] primarily because: (1) the process is self-contained without generating other wastes; (2) the flue gas essentially does not need to be cooled and reheated for desulfurization; (3) wet materials are not handled and water input requirements are minimal and (4) SO_2 and NO_x can be simultaneously removed. The dry regenerative process using an adsorbent involving physical adsorption can also produce salable sulfur byproduct.

The sorbents used in the dry regenerative FGD process are typically produced by impregnating porous $\gamma\text{-Al}_2\text{O}_3$ (as carrier material) with a solution of Cu or Ca salt which is then converted to CuO or CaO , referring to as the active material [5, 6]. Conventionally, the carrier material, $\gamma\text{-Al}_2\text{O}_3$, is prepared either directly from bauxite or from the monohydrate by dehydration or recrystallization at elevated temperature. Relative small surface area and poor attrition resistance are the two major disadvantages of the sorbents prepared by the conventional methods [7, 8]. The materials with a large surface area were traditionally *not* used as support because these materials usually have poor thermal stability and low mechanical attrition resistance. Sorbents with small surface area support will have a low SO_2 capacity. The attrition resistance is primarily determined by the support material structure (physical attrition) and interaction between the active species and support (chemical attrition).

Ceramic sorbents synthesized by the sol-gel method typically have rather high surface area [9]. Furthermore, the microstructure of the sol-gel derived ceramics consists of nanoscale crystalline particles bound strongly by necks of the same material formed through sintering. As a result, the sol-gel derived porous ceramic sorbents in pellet form are mechanically very strong, and expected to possess a high attrition resistance.

The sorption processes using metal oxides involve chemical reaction between SO_2 and the acceptor. Adsorbents based on physical adsorption mechanism, such as activated carbon [2, 3], have also been investigated for FGD. An ideal sorbent for SO_2 emission control must possess the following properties [10]: (1) high SO_2/CO_2 selectivity and high SO_2 capacity; (2) hydrophobicity, and (3) fast diffusion of SO_2 within the sorbent. Zeolites, the alumina silicate molecular sieves well known for their excellent sorption properties, have extensively been used in large scale adsorption and catalytic reaction processes [11-15]. Applications of zeolites in these areas are associated with their unique crystalline microporous pore structure, surface chemistry and mechanical strength. The strong mechanical attrition resistance of zeolites has been demonstrated by the successful application of several zeolites in large scale fluid catalytic cracking processes in petroleum refinery [14, 15].

Although zeolites have very good sorption properties for many gases, limited research efforts were reported on exploring zeolites for use as adsorbents for removal of SO_2 and NO_x for emission control [16-20]. This is obviously due to the concern of the relatively poor thermal stability and the hydrophilicity of zeolites. Most zeolites are not thermally and chemically stable at high temperatures and acidic environments typically encountered in FGD process. Water vapor in the flue gas can be more preferentially adsorbed by the hydrophilic zeolites, affecting adversely the SO_2 sorption properties of these zeolites [18, 19]. The thermal stability and hydrophobicity of a zeolite increase with the ratio of Si/Al in the zeolite framework. Among many synthetic and natural zeolites,

only two alumina-free zeolites are hydrophobic and thermally stable up to 1000°C: silicalite and the DAY zeolite, both of which are pure crystalline silica molecular sieves.

Silicalite was first synthesized by Union Carbide Co. in the later seventies [21]. It has a structure similar to ZSM-5 zeolite, with a framework consisting of intersecting channels defined by 10-membered oxygen rings. The channels have a near-circular cross-section of about 5 Å in diameter, wide enough to adsorb SO₂ molecules. Numerous studies on sorption and diffusion properties of organic gases and liquids in silicalite have been reported in the past decade [e.g., 21-24]. Gollakota and Chriswell [25] investigated the adsorption process using silicalite for FGD. They found that silicalite preferentially adsorbs SO₂ in the presence of major components of flue gas, such as water vapor, carbon oxides, oxygen and nitrogen. However, no detailed study on SO₂ sorption equilibrium and kinetics was reported by Gollakota and Chriswell.

The DAY zeolite was recently commercialized by a German company, Degussa AG. It is a dealuminated (aluminum free) Y zeolite synthesized by hydrothermal treatment of sodium Y zeolite with SiCl₄ [26, 27]. The DAY zeolite has the same structure as zeolite Y. The adsorption channels of the DAY zeolite, defined by 12 membered oxygen rings (connecting six basic sodalite units), have a near-circular cross-section of about 8 Å in diameter, larger than that of silicalite. As a result, the diffusivities of gases in zeolite Y are about two to three orders of magnitude larger than that in silicalite [13]. Between the two hydrophobic and thermally stable zeolites which have potential for use in FGD, the DAY zeolite appears to be superior to silicalite in terms of surface area and pore size. The SO₂ sorption capacity is directly proportional to the sorbent surface area while the diffusion resistance is inversely related to the pore size. No study regarding adsorption and diffusion of SO₂ and NO_X on the DAY zeolite was reported.

The main objectives of the research project in year four were to synthesize and characterize novel sol-gel derived alumina supported CuO and CaO sorbents for removing

SO₂ from flue gas; and to explore use of the hydrophobic zeolites as adsorbents or as sorbent support for FGD.

Technical Discussion

1. Adsorbent Synthesis and Characterization

Sol-gel method was applied to prepare alumina supported CuO or CaO FGD adsorbents as shown in *Figure 1*. Stable 1M boehmite sol (γ -ALOOH) was prepared using the Yoldas's process [39, 40]. The sol was synthesized by dissolving alumina-tri-secondary butoxide (97%, Janssen) in the deionized water at an initial temperature of 75 °C, and stirred vigorously. One liter of water was used per mole alkoxide. After heating at 90 °C for one hour, the resulting slurry with γ -ALOOH precipitates was peptized with HNO₃. In this study, 0.07 mole of 1M HNO₃ was added into 1 mole of sol according to Yoldas [41]. The peptized sol was refluxed at 90~100 °C for 10 hours, and a stable boehmite sol was obtained. The γ -alumina supports were prepared by drying a given amount of the boehmite sol in petri-dish under controlled conditions (air atmosphere, 40 °C and 60% humidity). The dried boehmite xerogel was calcined at 450 °C for 3 hours with a controlled heating and cooling rates [42]. Boehmite transformed to γ -alumina during the calcination [42~44].

Two methods were used to coat copper or calcium on the porous γ -alumina: wet-impregnation method and sol-solution mixing method. In the first method, a cuprous solution was synthesized by mixing cuprous chloride (CuCl) (Reagent ACS, Matheson Coleman & Bell Chemical Company), ammonia hydroxide (Reagent, ACS, Fisher Scientific), ammonia citrate (Reagent, Merck & CO. Inc.) and water with a given composition under controlled preparation conditions. Aqueous Cu(NO₃)₂, CuCl₂, Ca(NO₃)₂ or CaCl₂ solutions were prepared by dissolving Cu(NO₃)₂, CuCl₂, Ca(NO₃)₂ or CaCl₂ (ACS grade, Fisher Scientific) in water for coating copper or calcium into the alumina support. In coating the active species, the sol-gel derived γ -alumina supports, after heat-treated at 200 °C for several hours, were put into the solution containing active species or acceptor for more than 16 hours. The weight ratio of the active species to the support, calculated from the weights of support, volume and concentration of the active

species in the solution, was about 10~50%. The impregnated samples were dried in a vacuum oven at 200 °C under the flow of nitrogen (normally for 2 hours), and were then calcined in the furnace at 550 °C under air atmosphere for 6 hours to convert the active species into metal oxide.

The sol-solution mixing method was first reported by [45] to coat lanthanum on the grain surface of the γ -alumina support. In this method, a given amount of the copper or calcium salt solution was mixed with the boehmite sol. Extreme care was taken to avoid destabilizing the boehmite sol after the mixing of sol with the salt solution. The doped sol was dried at 200 °C under the atmosphere of nitrogen, and the resulting gels were calcined in the furnace at 550 °C under air atmosphere for 6 hours to convert the active species into metal oxide. This method has the advantage of being able to control precise amount of dopant.

According to the monolayer dispersion theory [32], about 66.5 wt.% of the CuO or 35 wt.% of CaO can be coated on the surface of γ -Al₂O₃ support with a BET surface area of 350 m²/g. It is very encouraging if the monolayer dispersion could be achieved in the preparation of FGD adsorbents since the loading amount of active species could be increased greatly, which in turn could enhance the adsorption capacity of SO₂ of the FGD adsorbents. Several CuO/ γ -Al₂O₃ and CaO/ γ -Al₂O₃ samples with various contents of metal oxide (10%~50%) were prepared by the wet-impregnation method to explore the possibility of monolayer coating, and to examine the effects of different preparation conditions on the properties of the final FGD adsorbents.

BET surface area, pore volume, pore size distribution and average pore size of the adsorbent samples were determined by nitrogen adsorption porosimeter (Micromeritics, ASAP 2000). The samples were first degassed at 150 °C under vacuum for more than 2 hours until the sample passed the degassing check-up test. The samples were then weighed and transferred to the testing port. The nitrogen adsorption and desorption isotherms were measured at liquid nitrogen temperature (78 °K) automatically. The

adsorption isotherm was used to calculate the BET surface area, pore volume, and the desorption isotherm was used to calculate the pore size distribution. X-ray diffractometer (Siemens, CuK α 1) was used to examine the phase structure of the adsorbent sample and to check the dispersion of active species on the support. The 2θ range used in the experiment was from 10° to 70° with a scanning speed of 3° per minute.

Five adsorbent samples prepared by the sol-gel methods are summarized in *Table 1*. The first sample is the pure γ -alumina without doping with active species. The second and the third samples are γ -alumina coated with cupric ion by the wet-impregnation method. The difference in these two samples is that the copper-1 sample was prepared from cupric chloride and copper-2 was prepared from cupric nitrate. These two samples were prepared primarily for the purpose of examining the effect of different sources of copper on the final properties of the adsorbent. The fourth and the fifth samples were coated with calcium using the wet-impregnation method and the solution-sol mixing method, respectively. These samples were prepared to examine the effects of the different coating methods on the final results.

The nitrogen adsorption isotherms of all the five samples are of type IV [46], as shown in *Figure 2*. The desorption hysteresis loop indicates that these adsorbents are mesoporous. *Figure 3* shows the pore size distributions (determined from nitrogen desorption isotherms) for adsorbent Calcium-1. The BET surface area, pore volume, average pore size and pore size distribution range for these five adsorbents are summarized in *Table 2*. All adsorbent samples have a narrow pore size distribution with an average pore diameter of around 4 nm. The surface area of these samples is large.

CuCl , CuCl_2 and CaCl_2 coated alumina adsorbents were prepared with different loading amount of the active species. The adsorbents prepared are summarized in *Table 3* with their pore structure data. The adsorbents (Copper-3, Copper-4, Copper-5, Copper-6) with CuCl as the precursor, prepared by a unique method recently developed in this laboratory [9], have a much higher surface area. Although the BET surface areas based

on the total weight of adsorbents for the other adsorbents (Copper-7, Copper-8, Copper-9, Copper-10 and Calcium-3, Calcium-4) decrease with the increasing loaded amount of the active species, the corrected BET surface areas based on the weight of pure alumina in adsorbents for those samples are essentially constant. This is consistent with the monolayer dispersion theory which predicts a relatively constant surface area of adsorbents until a critical loading amount. That corrected BET surface area of Calcium-5 is smaller than that of pure alumina is probably because the loading amount of active species exceeds the critical value. These FGD samples were heated in air at 550 °C for 6 hours to convert the active species from salt to metal oxide which is dispersed on the grain surface of alumina support.

The pore texture data of these FGD adsorbents with metal oxide active species are summarized in *Table 4*. Since the loading of CuO in CuO samples reported in *Table 4* has not exceeded the critical value of the monolayer coating, the active species is expected to be dispersed on the surface of the alumina in a monolayer or sub-monolayer form. This was verified by the XRD data of these samples shown in *Figure 4 (A)* and *(B)*. No sharp XRD reflection peaks are observed for these samples. The sol-gel derived γ -alumina, although having a cubic crystalline structure, is known to have very weak x-ray reflection peaks [43, 44, 47]. From these XRD data it is obvious that no other XRD detectable crystallites are present in these samples. This suggests that the active species is more likely present in the form of two-dimensional layer (possibly monolayer) on the grain surface of the γ -alumina support [32].

The uniform pore size and large surface area of these adsorbent samples are a result of the unique characteristics of the sol-gel processing. The surface area of the copper or calcium coated samples is smaller than that of the pure γ -alumina. Coating the active species also changes the average pore size and pore volume of the alumina adsorbents. Comparing the pore texture data of copper-1 and copper-2 leads to the conclusion that different source of active species has negligible effects on the pore texture

of the final product prepared by wet-impregnation method. These suggest that the same sol synthesis and coating method will give essentially same pore structure regardless of different active species. Comparing the two calcium coated samples prepared by the different coating methods, the sol-solution mixing method yields an adsorbent with smaller surface area, pore volume and average pore size. This is a result of the phenomenological difference in these two coating methods [9].

In the wet-impregnation coating method, the microstructure of the support (γ -alumina) has already been consolidated after the calcination step. Once the support is brought to contact with the impregnating solution, active species is adsorbed on the surface of the support and remains on the support surface after the solvent is removed during the drying step. Therefore, wet-impregnation does essentially not change the microstructure of the support. The sol-solution mixing method, developed initially for coating oxide layer on the grain surface of ceramic membranes for other property improvement [45, 48], works in a very different fashion. In this method, stable boehmite sol is mixed with an active species containing salt solution. After mixing, the active species can be coated on the grain surface of the sol particles either during the sol aging step or drying step. However, mixing a salt solution into the boehmite sol may change the pH and ion (cation and anion) concentrations of the sol, which, if not well controlled, may destabilize the sol, resulting in the formation and precipitation of larger aggregates. In this work, mixing procedure and conditions were carefully controlled so that the boehmite sol remained stable after being doped with silver containing salt solution. Some other species could also be coated on the grain surface of the sol particles [48], but experiments performed in this laboratory showed that mixing cuprous salt solution with the boehmite sol destabilized the sol, yielding a final product with a small surface area (< 90 m^2/g).

Although the calcium salt doped boehmite sol remained stable, the slight change in the pH and ion concentrations after the doping still altered the size and shape of the

primary particles. Thus, the difference in the microstructure of the two silver coated adsorbents is primarily due to the different primary particle size and shape, which, together with the their packing pattern and extent of consolidation, determine the pore structure of the final product. Despite that the adsorbent prepared by the sol-solution mixing method has a smaller surface area, this method allows accurate control of the dopant concentration and eliminates the additional drying step required in the wet-impregnation coating method.

2. Stability Tests of FGD Adsorbents

The thermal and chemical stability of the adsorbents prepared were investigated by comparing the initial pore and phase structure of the sample to that after heat-treatment under various atmospheres. The following are the conditions on which the adsorbents were heat-treated :

Condition 1. Calcination

Temperature : (1). From 25 °C to 550 °C at the heating rate of 30 °C/hour.
(2). Heated at constant temperature of 550 °C for 6 hours.
(3). From 550 °C to 350 °C at the cooling rate of 30 °C/hour.
(4). From 350 °C to 25 °C at the cooling rate of 100 °C/hour.

Atmosphere : Air

Condition 2. : Sintering

Temperature : (1). From 25 °C to 850 °C at the heating rate of 30 °C/hour.
(2). Heated at constant temperature of 850 °C for 168 hours.
(3). From 850 °C to 350 °C at the cooling rate of 30 °C/hour.
(4). Cooled from 350 °C to 25 °C at the rate of 100 °C/hour.

Atmosphere : Air

Condition 3: Sulphation Treatment

Temperature : 850 °C (or 550 °C)

Total flow rate : 552 ml/min

Atmosphere : 2.2% SO₂, 97.8% Air

Duration : 60 hours in the first treatment, 2 hour in the subsequent cycles.

Condition 4: Sulphation under Humid Atmosphere

Temperature : 850 °C

Total flow rate : 309 ml/min

Atmosphere: 2.0% SO₂, 12% H₂O (vapor), 86% Air

Duration : 60 hours

Condition 5: Regeneration

Temperature : 850 °C

Total flow rate : 205 ml/min

Atmosphere: 34.1% H₂, 55.9% Air

Duration : 2 hours

Condition 6: Oxidation

Temperature : 850~550 °C (The temperature was first decreased from 850 °C to 550 °C by natural cooling and was then kept at 550 °C)

Total flow rate : 540 ml/min,

Atmosphere: Air

Duration : 2 hours

The color of the freshly prepared Copper-1 and Copper-2 samples is blue or green, typical color of cupric chloride or cupric nitrate. After the calcination heat-treatment (Condition 1) , the color of the copper samples became black/green, the color of CuO. The BET surface area of these two copper samples decreases after the heat-treatment at 550 °C as shown in *Table 2*. These results suggest that CuCl₂ and Cu(NO₃)₂ coated on the alumina support surface converted to CuO after the heat treatment at 550 °C for 6 hours. CaCl₂ and CaO should look white, so no color change is expected for calcium coated samples. It is believed the coated calcium active species had also converted to CaO after the heat treatment at 550 °C for 6 hours.

For the four CuO or CaO coated samples, the surface area and pore volume decreased and the pore volume increased after sintering at 850 °C (Condition 2) as shown in *Table 5*. This is due to the sintering effects on the γ -alumina supports prepared by the sol-gel method. Nevertheless, the final surface areas of these CuO and CaO samples are still fairly large as compared with the conventional FGD sorbents. These surface area data are also consistent with the results reported by Duisterwinkel et al. [28] for the similar sorbents prepared by the sol-gel method. It should be pointed out that application temperature of these sorbents for FGD is below 500°C, much lower than the heat-treatment temperature used in this study (850°C). So these sorbents should be very stable in practical applications in FGD.

The purpose of the chemical and hydrothermal stability tests is to evaluate the stability of the structure of the adsorbents under severe environments. The treatments conditions used in this study were much more caustic than the application environments of these adsorbents in the FGD process. It is believed that if the pore structure of adsorbents is stable in these severe conditions, it is more stable in less severe atmosphere.

The pore structure of the adsorbents after the first sulphation treatment at 850 °C for 60 hours (Condition 3) is summarized in *Table 6*. As compared with the data given in *Table 2*, the data presented in *Table 2* and *4* indicate that for all samples the BET surface area and pore volume decreased, and the pore size range and average pore size increased after the sulphation treatment. This is because of the effects of both chemical reaction and sintering on the materials. It is believed that the main contribution to the pore structure changes during this sulphation treatment came from the sintering effects. Although the surface area of all these adsorbents decreased substantially after the sulphation treatment at 850 °C, the samples prepared in this study still have a much larger surface area than γ -alumina supported CaO adsorbents reported for the FGD process [29].

The pore structure data of the same CuO or CuO coated adsorbents listed in *Table 6* after additional 4 cycles of sulphation-reduction-oxidation (Condition 3, Condition 5,

and Condition 6) are given in *Table 7*. Comparing to the data given in *Table 6*, the pore structure of these adsorbents after the sulphation-reduction-oxidation cycles was essentially unchanged. This suggests that the first sulphation treatment at 850 °C for 60 hours stabilized the pore structure of the adsorbents. It is certain that the pore structure of the adsorbents will be stable after many more sulphation-regeneration-oxidation cycles at lower temperatures.

The pore texture data of the same FGD adsorbents after additional treatment of sulphation under humid atmosphere (Condition 4) are listed in *Table 8*. The environment encountered in this treatment was the most caustic, but only small changes of the pore structure of the FGD adsorbents after this treatment are observed if one compares these results with the pore texture data in *Table 6* and *7*. This indicates that the FGD adsorbents prepared in this study are stable in the humid environment.

Thermal, hydrothermal and chemical stability tests of the DAY and silicalite zeolites adsorbents have been carried out at 850 °C. Nitrogen adsorption and XRD were employed to measure the pore texture data and phase structure of these zeolites samples before and after treatments. As shown in *Table 9*, the pore texture of the DAY zeolites and silicalite are essentially the same after these treatments. The XRD results (*Figure 5* and *6*) also show that the phase structure of these zeolites had no detectable changes. These experimental results lead to the conclusion that the hydrophobic zeolites (the DAY zeolite and silicalite) tested in this work are very stable in different atmospheres up to 850 °C. This conclusion will be further verified by the adsorption data presented next. These data suggest that both silicalite and the DAY zeolite are suitable candidate of adsorbents (physical adsorbent) or adsorbent support for FGD at high temperatures.

3. Adsorption / Desorption of SO₂ in Zeolite Adsorbents

The adsorption of SO₂ on the DAY zeolite and silicalite were performed with a flow-through method in the Cahn balance system at temperatures of 25, 50 and 100 °C. About 150 mg of DAY zeolite powder or silicalite powder sample was used in the adsorption experiments. The adsorbent was first activated at high temperature (550 °C) and vacuum (<10⁻¹ mmHg) for more than 10 hours, it was then cooled under the flow of air. After the desired temperature was reached, SO₂ was introduced to the system at a given rate to achieve a given concentration (0.5%~5%). The total pressure of the balance system was 1 atm. The weight change of the adsorbent was monitored and recorded by the computer. Adsorption equilibrium was established when the weight of the sample became constant. It was found that the adsorption amount of air on both silicalite and the DAY zeolite are very small comparing with the adsorption amount of SO₂ on zeolites, so it is reasonable to consider the air as an inert component. The air was used as inert carrier instead of helium because the constituent of this adsorbate gas is more close to flue gas.

The adsorption isotherms of SO₂ on these two zeolites, as plotted in *Figure 7* and 8, can not be characterized as type I isotherm, suggesting a different adsorption mechanism. The SO₂ sorption amount at SO₂ pressure of 25 mmHg on these two zeolites are summarized in *Table 10* together with some other characteristics of these zeolites. In the SO₂ partial pressure range tested in this work, larger adsorption amount of SO₂ was obtained on silicalite than on the DAY zeolite. This suggests that the molecular interaction between SO₂ with silicalite surface is more stronger than that between SO₂ and the DAY zeolite. This can be verified by the heat of adsorption data listed in *Table 11*. The mechanism of the adsorption of SO₂ on zeolite deserves further theoretical investigation.

All the adsorption isotherms of SO₂ on the DAY zeolite and silicalite can be well correlated by the Freundlich adsorption isotherm equation :

$$\Gamma = KP^{1/n}$$

where Γ is the adsorbed amount (mmol/g), P is the pressure of gas phase (mmHg), K and n are the two equation constants. A comparison of isotherms calculated from Freundlich equation and the experimental data are shown in *Figure 7* and *8*. The regressed Freundlich equation constants are listed in *Table 11* for all isotherms. The heat of adsorption for both adsorbents were calculated from the equation constant K, which is correspondent to Henry's constant, by the van't Hoff equation :

$$\frac{\partial \ln K}{\partial T} = -\frac{(-\Delta H)}{RT^2}$$

In general, adsorption data at low pressure and high temperature can provide accurate information about the interaction between adsorbate and adsorbent. The heat of adsorption of SO_2 on the DAY zeolite and silicalite are 6.9 and 16.9 kJ/mole, respectively. The small heat of adsorption on the DAY zeolite at low SO_2 pressure is consistent with the adsorption amount of SO_2 which is smaller on the DAY zeolite than on silicalite. The DAY zeolite has a larger BET surface area and larger pore volume, but its adsorption affinity to SO_2 is not as strong as that of silicalite to SO_2 at low concentration range. It's very interesting to point out that Freundlich equation was also used to successfully describe the adsorption equilibrium of SO_2 on activated carbon [49] and polymer resin adsorbent [10].

The experimentally measured SO_2 uptake curves ($W(t)/W_\infty$ vs t) on these two zeolites in short time period can be described by the equation :

$$(W(t)/W_\infty)^2 = kt$$

where k is a rate constant. If the pore diffusion is the rate-limiting step, k can be correlated to the diffusivity of SO_2 in the micropore by:

$$k = 36D_C/\pi r_C^2$$

Experimentally measured values of k for SO_2 in these two zeolites low SO_2 partial pressure and three different temperatures are given in *Table 10*. Values of k obtained in this work are essentially the same for both zeolites. It is known that diffusivity of gas in the DAY zeolite ($10^{-8} \text{ cm}^2/\text{s}$) should be 2 to 3 orders of magnitude larger than that in silicalite. If the pore diffusion was the rate-limiting step, much smaller values of k should be observed for silicalite than the DAY zeolite if both zeolites have the same crystallite size. These results suggest that sorption of SO_2 on the internal pore surface of the zeolites is the rate-limiting step. The activation energy of the adsorption rate, calculated from k at different temperatures, for both zeolites (14.6 for the DAY zeolite and 13.8 for the silicalite) are almost the same at low SO_2 partial pressure. This strongly suggests that the sorption on surface is the rate-limiting step.

The adsorption equilibrium amounts of SO_2 at 5% SO_2 concentration on the silicalite samples which have been thermally treated at 550°C , or 850°C , or hydrothermally treated at 850°C were measured to check the changes of adsorption ability of these samples. As shown in *Table 12*, the equilibrium adsorption amount of SO_2 at 5% SO_2 concentration on silicalite decreased slightly with the proceeding of the heat treatments. The rate of adsorption on the thermally and hydrothermally treated samples are the same as that on the fresh sample. It was estimated from the stability model proposed by Suckow et al. [50] that the silicalite sample will decrease 50% of the activity after application in FGD process at 200°C for 9 years. This indicates that silicalite adsorbent has a very good thermal and hydrothermal stability.

The adsorption of SO_2 was also measured on silicalite sample which was first exposed to water vapor for 1 hour. The adsorption amount of SO_2 decreased by about 20% from 1.73 mmole/g to 1.37 mmole/g at SO_2 partial pressure of 30 mmHg. The adsorption amount of water was about 0.44 mmole/g in this case. This result shows that the presence of water vapor in the flue gas exhibits effect on the physical adsorption properties of silicalite.

4. Sulphation and Regeneration on Alumina Supported FGD Adsorbents

About 300.0 mg of a CuO or CaO FGD adsorbent was put in the sample pan for sulphation and regeneration experiment. The fresh FGD adsorbent samples put in the reactor tube were heated to the desired temperature (i.e. 550 °C) under the flow of air (50 ml/min) at 1 atm. When the baseline of the balance became flat, indicating that balance was stabilized and ready for taking data, the flow rate of air was then increased to desired value (about 500 ml/min in this study), and nitrogen (50 ml/min) purge stream was introduced into the system from the top of the balance. SO₂ was then introduced to the reactor tube at a controlled flow rate. The concentration of SO₂ in the flue gas for sulphation in this work was about 5~10 %. In regeneration step, the sulphated adsorbent was first heated to the desired temperature under the flow of nitrogen at flow rate of 50 ml/min from both top and bottom of the balance. The flow rate of nitrogen was adjusted to about 300 ml/min and hydrogen was introduced at flow rate of 30 ~ 60 ml/min after the baseline of the balance became stable. The concentration of hydrogen in the reducing gases for regeneration was about 10~20 %. The results on the sulphation and regeneration on a CuO sorbent and a CaO sorbent are shown in *Figure 9~12*. Specific conditions for sulphation and regeneration are also presented in *Figure 9~12*.

As shown by the data listed in *Table 13*, the equilibrium uptake on the CuO sorbent synthesized in this lab (45 wt%) is much larger than that (7.0 wt%) on the CuO sorbent reported in literature. The difference in the temperature and SO₂ concentration in gas stream may contribute to the different SO₂ capacity on the both CuO sorbents compared. However, the larger SO₂ sorption capacity for the sol-gel derived CuO sorbent is mainly due to the fact that the sol-gel derived sorbent synthesized in this lab has a larger surface area and high CuO loading. The SO₂ to CuO molar ratio on the sorbent synthesized in this lab is also larger than that on the sorbent reported in literature, suggesting that CuO is better dispersed on the grain surface of the sol-gel derived alumina

support. SO_2 sorption rate on the sol-gel derived CuO sorbent is also larger than that on the CuO sorbent reported in the literature as indicated in *Table 13*.

Sulphation uptake curve on a CaO sorbent (Calcium-3) at 850 $^{\circ}\text{C}$ is shown in *Figure 10*. The sulphation rate on Calcium-3 is faster than the reported value on α -alumina supported CaO FGD adsorbents. 10 % weight gain was obtained in 45 minutes in Calcium-3, while 68 minutes are needed to uptake 10 % SO_2 in the literature (Centi et al., 1992a).

The regeneration kinetics were also measured for the sulphated Copper-4 and Calcium-3. The regeneration curves for Copper-4 and Calcium-3 are plotted in *Figure 11* and *12*. Compared with the regeneration kinetics on a commercial CuO adsorbents reported in the literature, the sulphated Copper-4 FGD adsorbent has a fast regeneration rate as shown in *Table 14*. Only 10 minutes are needed to recover 90% of the activity of for Copper-4 FGD adsorbent, compared to 20 minutes are needed for commercial copper oxide FGD adsorbents as reported by Harriot and Markussen [30]. Regeneration of sulphated Calcium-3 is relatively difficult and more reducing environment is needed to recover full activity. This is partly because CaS formed in the sulphation stage is more difficult to decompose [29].

A very simple method was established to measure the concentration of active species or acceptor (CuO or CaO) in the FGD adsorbents prepared in this work by the Cahn balance system. After the adsorbent was reduced to element copper or calcium in the sulphation-reduction-oxidation cycles, the oxidation was carried out at the same temperature as regeneration. The weight gain curve was recorded and the maximum weight gain was used to calculate the content of the active species. The concentration of CuO in Copper-1 measured by this method is 9.7% which is very close to the value estimated from the amount of chemicals used in preparing the sample (10%). So this method will be applied to determine the concentration of active species in the FGD adsorbents prepared in the future.

Marketing/Commercialization Discussion

The commercialization of the dry sorption FGD process employing the γ -alumina supported CuO or CaO FGD adsorbents developed in this work is primarily dependent on the large scale production of the adsorbent. This is because the regenerative dry sorption FGD processes using metal oxide sorbent has already been commercialized as Shell FGD process in 1970's [51] and have been intensively investigated and modified in both laboratory and pilot scale in several DOE funded research projects [3, 8, 52, 53]. The key point to improve the performance of this process is to develop new adsorbents which have superior adsorption, regeneration and mechanical properties. The sol-gel prepared γ -alumina supported CuO or CaO FGD adsorbents developed in this work appear to possess better adsorption properties and improved mechanical strength. The use of these adsorbents may improve the performance of the commercial dry sorption FGD process.

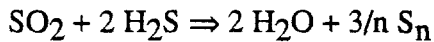
1. Commercialization of Adsorbent Production

The production of adsorbent or catalysts in a large scale is a highly technical work in industry. The application of sol-gel technique to the synthesis of new type of adsorbent is still in its infancy. Sol-gel method was applied to prepare spherical silica bead as catalyst support. [34] The sol-gel method was also used to make silica based zeolite pellet. [54, 55]. The processes for production of spherical silica bead and binderless zeolite has been commercialized respectively by Shell [34], and Nanjian Refinery (P. R. China) [55]. The large scale production of spherical γ -alumina supported CaO FGD adsorbent has been reported recently [56]). These techniques will be extended to prepare spherical γ -alumina supported CuO FGD adsorbents in year five of OCDO research program. The sol-gel prepared spherical γ -alumina supported CuO FGD adsorbent is expected to have good adsorption and regeneration properties, and good mechanical properties.

2. Recovery of SO₂ from FGD Process

The USA consumed over 11 millions tons of sulfur in 1988 [52]. Most of the them was produced by steaming injection into underground deposits using the thermally inefficient Frassch process. SO₂ generated from natural gas and petroleum processing was another large source. Due to the dwindling of the capacity of the sulfur deposit and production of sulfur from natural gas and petroleum, other alternatives of elemental sulfur production such as sulfur recovery from flue gas or other tailgas by Claus or modified Claus process is becoming more attractive. Furthermore, the recovery of sulfur from flue gas offers an alternatives to flue gas treatment processes that produce large volume of throwaway waste that must be disposed of in an environmentally safe manner.

The Claus process is based on the following reaction :



In a sorption based FGD process, about 90% of SO₂ (2000~3000 ppm) in the flue gas after electric precipitator is taken by the dry solid sorbent (copper oxide) in the sulphation step at 300 ~ 450 °C . The clean gas with SO₂ content of about 200 ppm is released to the atmosphere. After regeneration with reducing gas, the adsorbed SO₂ in the sorbent would be released in the regeneration-off gas with a high concentration (about 40 vol. %). The SO₂ in the regeneration-off gas can be recovered either by the Claus process to generate elemental sulfur or recovered by PSA process to produce concentrated SO₂ which can be easily converted to sulfuric acid.

McCrea et al. [57] have designed a process to remove and recover SO₂ from flue gas by copper oxide for 250 Mw power plant. The conceptual process flow sheet of this FGD process is shown in *Figure 13*. Flue gas (25.9 million scfh for each module) containing 0.215 vol% SO₂ is removed from the boiler after steam economizer and is routed through an electrostatic precipitator to remove the solid particles. The gas then passes the fluidized reactor where 90% of the SO₂ is removed. The clean gas is then returned to the air preheater. Pellet sorbent containing 1.0 g of sulfur per 100 g sorbent

enter the reactor at a rate of 305,000 1b/hr and leave containing 2.5 g sulfur per 100 g sorbent. Flue gas enters the reactor at 300 °C and pellet sorbents enter at 465 °C. Both leave at 330 °C. Solids leave the reactor at a rate of 317,000 1b/hr and are fed to a fluidized heat-exchanger to increase their temperature to 445 °C. The solid are then conveyed to the regenerator where CH₄ is fed at a rate of 31,300 scfh at a temperature of 400 °C. The regenerated sorbents containing 1.0 g of sulfur per 100 sorbent are fed to the adsorber/reactor at a rate of 303,000 1b/hr. The gaseous products leaving the regenerator contain 38 vol% of SO₂ and are fed to the Claus process to recover sulfur. The major operation conditions are listed on the flow sheet (*Figure 13*).

Table 15 presents the rates and compositions of the major process streams for this process. The estimated operating cost for this FGD process is \$11,339,800 for a 1000 Mw power plant. According to Dautzenberg et al. [51], the total operating costs for Shell's FGD process after credit for sulfur (\$30/ton) are about \$200/ton sulfur removed. The capital cost for Shell's FGD process is between \$26~30/kw, depending on the capacity of the power plant. The operating cost of adsorption FGD process can be substantially reduced if the attrition loss of the adsorbent is minimized and sulphation and regeneration are carried out at same temperature (400~450 °C) (McCrea et al., 1970).

Compared with the commercial sorbents, the sorbents developed in this work have a high adsorption capacity, faster sorption/regeneration kinetics and strong mechanical strength. So it is expected that the operating costs of the FGD process employing the adsorbents developed in this work will be less than \$200/ton of sulfur removed.

3. Future Work Plans

In order to improve the mechanical properties of the alumina supported FGD adsorbents developed in this work and to promote the commercial application of this new type of adsorbent, a follow-up research program to continue the work in year four was proposed for year five and was funded by OCDO. γ -Alumina bead with regular shape,

preferentially sphere, will be fabricated by the sol-gel method and used to prepare FGD adsorbents. The DAY zeolite will be used as a support to prepare supported CuO or CaO adsorbents to explore the possibility of application of zeolite as FGD adsorbent or support. The mechanical properties including crushing strength, physical attrition rate of the FGD adsorbents synthesized in this work will be measured. Adsorption and regeneration of SO₂ on the DAY zeolite supported CuO or CaO adsorbents will be studied in the Cahn balance system. Several selected FGD adsorbents prepared in this work will be tested in fixed-bed reactor and fluidized-bed reactor for their FGD performance in removing SO₂ from the simulated flue gas.

Literature Cited

1. D.S. Henzel, B.A. Laseke, E.O. Smith and D.O. Swenson, "Handbook for Flue Gas Desulfurization Scrubbing with Limestone", Noyes, Park Ridge, NJ (1982)
2. M. Satriana, "New Developments in Flue Gas Desulfurization Technology", Noyes, Park Ridge, NJ (1981)
3. J. T. Yeh, C.J. Drummond and J.I. Joubert, "Process Simulation of the Fluidized-Bed Copper Oxide Process Sulfation Reaction," *Environmental Progress*, 6, 44 (1987)
4. H.C. Frey, "Performance Model of the Fluidized Bed Copper Oxide Process for SO₂/NO_x Control," Presented at 86th Annual Meeting and Exhibition, Denver, Co. June 13-18 (1993)
5. N.L. Cull, "Flue Gas Desulfurization Sorbent," *U.S. Patent*, 4,085,195 (1978)
6. A.E. Duistewinkel, "Clean Coal Combustion with *in-situ* Impregnated Sol-gel Sorbent", Ph.D. Thesis, Delft University of Technology, Delft, the Netherlands (1991)
7. W.W. Hedges and J. T. Yeh, "Kinetics of Sulfur Dioxide Uptakes on Supported Cerium Oxide Sorbents," *Environmental Progress*, 11, 98 (1992)
8. J.T. Yeh, R.J. Demski, J.P. Strakey and J.I. Joubert, "Combined SO₂/NO_x Removal from Flue Gas", *Environmental Progress*, 4, 223 (1985)
9. S.G. Deng and Y.S. Lin, "Sol-gel Preparation of Alumina Adsorbents for Gas Separation", *AIChE J.*, in press (1994)
10. E. S. Kikkinides and R.T. Yang, "Gas Separation and Purification by Polymeric Adsorbents : Flue Gas Desulfurization and SO₂ Recovery with Styrenic Polymers," *Ind. Eng. Chem. Res.*, 32, 2365 (1993)
11. D.W. Breck, "Zeolite Molecular Sieves", Wiley, New York (1974)

12. D.M. Ruthven, "Principle of Adsorption and Adsorption Processes", Wiley, New York (1984)
13. J. Karger and D.M. Ruthven, "Diffusion in Zeolites and Other Microporous Solids", Wiley, New York (1992)
14. N.Y. Chen, "Shape Selective Catalysis at the 30-Year Mark", *ACS Symp. Seri.*, 368, 468 (1988)
15. A. Corma, in "Zeolites, Facts, Figures and Future", (Eds.) P.A. Jacobs, R.A. van Santen, Elsevier, Amsterdam, p.49-68 (1989)
16. J.C. Gupta, Y.H. Ma and L.B. Sand, "Diffusion of Sulfur Dioxide in a Synthetic Mordenite and a Natural Erite," *AIChE Symp. Series*, 67 (117), 51 (1971)
17. Y.H. Ma and A.J. Roux, "Multicomponent Rates of Adsorption of SO₂ and CO₂ in Sodium Mordenite," *AIChE J.*, 19, 1055 (1973)
18. A. Roux, A.A. Huang, Y.H. Ma and I. Zwiebel, "Sulfur Dioxide Adsorption on Modenites," *AIChE Symp. Series*, 69 (134), 46 (1973)
19. Y.H. Ma, R.J. Byron, P. Feltri and T.Y. Lee, "Effects of Presorbed Water Vapor upon the Sorption and Diffusion of SO₂ in Natural Modenites," *AIChE Symp. Series*, 74 (179), 48 (1978)
20. H.G. Stenger, jr., K. Hu and D.R. Simpson, "Chromatographic Separation and Concentration of Sulfur Dioxide in Flue Gas," *Ind. Eng. Chem. Res.*, 32, 2736 (1993)
21. E.M. Flanigen, J.M. Bennett, R.W. Grose, J.P. Cohen, R.L. Patton, R.M. Kirchne and J.V. Smith, "Silicalite, a New Hydrophobic Crystalline Silica Molecular Sieve", *Nature* (London), 271, 512 (1978)
22. Y.S. Lin and Y.H. Ma, in "Zeolites, Facts, Figures and Future", (Eds.) P.A. Jacobs, R.A. van Santen, Elsevier, Amsterdam, p.877-86 (1989)

23. Y.S. Lin and Y.H. Ma, "Liquid Diffusion and Adsorption of Aqueous Ethanol, Propanols and Butanols in Silicalite by HPLC", *ACS Symp. Series*, 368, 452 (1988)
24. Y.H. Ma and Y.S. Lin, "Adsorption of Liquid Hydrocarbons in Silicalites," *AIChE Symp. Series*, 81 (242), 39 (1985)
25. S.V. Gollkota and C.D. Chriswell, "Study of an Adsorption Process Using Silicalite for Sulfur dioxide Removal from Combustion Gases," *Ind. Eng. Chem. Res.*, 27, 139 (1988)
26. Degussa, "Wessalith DAY, a Hydrophobic Zeolite for Gas Purification". Technical Report 4307.1, Degussa, Frankfurt, Germany (1992)
27. E. Gail, "Dealuminized Y-Zeolites, Properties and Applications", paper 183g, Presented at 1993 AIChE Annual Meeting, November 7-11, St. Louis (1993)
28. A.E. Duisterwinkel, E.B. M. Doesburg and G. Hakvoort, "Comparing Regenerative SO_2 Sorbents Using TG : The SRO Test," *Thermochim. Acta*, 141, 103 (1989)
29. G.C.M. Hakvoort, J.C. van der Bleek, J.C. Schouten, P.J.M. Valkenburg, "The Study of Sorbent Material for Desulfurization of Combustion Gases at High Temperature," *Thermochim Acta*, 114, 103 (1987)
30. P. Harriott and J.M. Markussen, "Kinetics of Sorbent Regeneration in the Copper oxide Process for Flue Gas Cleanup," *Ind. Eng. Chem. Res.*, 31, 373 (1992)
31. G. Centi, A. Riva, N. Passarini, G. Brambilla, B.K. Hodnett, B. Delmon and M. Ruwet, "Combined $\text{DeSO}_2/\text{DeNO}_x$ Reactions on a Copper on Alumina Sorbent-Catalyst 1. Mechanism of SO_2 Oxidation-Adsorption", *Ind. Eng. Chem. Res.*, 31, 1947 (1992)
32. Y.-C. Xie and Y.Q. Tang, "Spontaneous Monolayer Dispersion of Oxides and Salts onto Surface of Supports: Applications to Heterogeneous Catalysis," *Advances in Catalysis*, 37, 1(1990)

33. Y. Xie, N. Bu, J. Liu, G. Yang, J. Qiu, Y. Tang, "Adsorbents for Use in the Separation of Carbon Monoxide and/or Unsaturated Hydrocarbons from Mixed Gases," *US Patent* 4,917,711 (1990)
34. Spek, T.G. and M.J.L. van Beem, " Silica Particles and Method for their Preparation," *European Patent* 0067459 A1 (1982)
35. P.K. Doolin, "Laboratory Testing Procedure for Evaluation of Fluidized Bed Catalyst Attrition," *J. Testing and Evaluation*, 21, 481 (1993)
36. J.H.A. Kiel, W. Prins and WPM van Swaaij, "Performance of Silica Supported Copper Oxide Sorbents for SO₂/NO_x Removal from Flue Gas," *Appl. Catal. B. Environmental*, 1, 13 (1992)
37. Y.S. Lin and Y.H. Ma, "A Comparative Chromatographic Study of Liquid Adsorption and Diffusion in Microporous and Macroporous Adsorbents," *Ind. Eng. Chem. Res.*, 28, 622 (1989)
38. Y.S. Lin, "Adsorption and Diffusion of Liquids in Porous Solids", Ph.D. Thesis, Worcester Polytechnic Institute, Worcester, MA (1988)
39. Yoldas, B. E., "Transparent Porous Alumina," *Amer. Ceram. Soc. Bull.*, 54, 286 (1975)
40. Yoldas, B. E., "Alumina Sol Prepared from Alkoxides," *Amer. Ceram. Soc. Bull.*, 54, 289 (1975)
41. Yoldas, B. E., "Transparent Porous Alumina," *Amer. Ceram. Soc. Bull.*, 54, 286 (1975)
42. Leenaars, A. F. M., K. Keizer, and A. J. Burggraaf, "The Preparation and Characterization of Alumina Membrane with Ultrafine Pores," *J. Mater. Sci.*, 19,1077(1984)
43. Wilson, S. J., "Phase Transformation and Development of Microstructure in Boehmite-Derived Transition Alumina, " *Proc. British Ceramic Soc.*, 28, 281 (1979)

44 Wilson, S. J, "The Dehydration of Boehmite, γ -ALOOH, to γ -Al₂O₃," *J. Solid State Chem.*, 30, 247 (1979)

45 Lin, Y. S., K. J. de Veries, and A. J. Burggraaf, "Thermal Stability and Its Improvement of the Alumina Membrane Top-Layers Prepared by Sol-Gel Methods," *J. Mat. Sci.*, 26, 715 (1991)

46 Gregg, S. J., and K. S. W. Sing, *Adsorption, Surface Area and Porosity*, Academic Press, London, Second Edition (1982)

47 Wefers, K., and C. Misra, "Oxides and Hydroxides of Alumina," *Alcoa Technical Paper 19*, Revised, Alcoa Center, Penn (1987)

48 Lin, Y. S., C.-H. Chang, and R. Gopalan, "Improvement of Thermal Stability of Porous Nano-Structured Ceramic Membranes," *Ind. Eng. Chem.*, in press (1994)

49 Gray, P. G., and D. D. Do, "Adsorption and Desorption Dynamics of Sulfur Dioxide on a Single large Activated Carbon Particles," *Chem. Eng. Comm.*, 96, 141 (1990)

50 Suckow, M., W. Lutz, J. Kornatowski, M. Rozadowski, and M. Wark, "Calculation of the Hydrothermal Long-Term Stability of Zeolites in Gas-Desulphurization and Gas-Drying Processes," *Gas Separation & Purification*, 6, 101 (1992)

51 Dautzenberg, F. M., and J. E. Nader, "Shell's Flue Gas Desulphurization Process," *Chem. Eng. Progress*, 67(8), 87 (1971)

52 Gangwal, S. K., W. J. McMichael, and T. P. Dorchak, "The Direct Sulfur Recovery Process," *Envirn. Progress*, 10(2), 186 (1991)

53. Ma, W. T., and J. L. Haslbeck, "NOXSO SO₂/NO_x Flue Gas Treatment Process : Proof-of-Concept Test," *Envir. Progress*, 12, 163 (1993)

55 Li, S. A., et al., "The Process for the Preparation of Zeolite Molecular Sieve Type A in the form of Binderless Spherical Granules," *Chinese Patent* 87105499 (1990)

56 Wolff, E. H. P., A. W. Gerritsen, and P.J. T. Verheijen, "Attrition of an Alumina-Based Sorbent for Regenerative Sulphur Capture from Flue Gas in a Fixed Bed," *Powder Technology*, **76**, 47 (1993)

57 D. H. McCrea, A. J. Froney, and J. G. Myers, "Recovery of Sulfur From Flue Gases Using a Copper Oxide Adsorbent," *J. Air Pollution Control Association*, **20**, 819 (1970)

58 Wu, P., A. Debebe, and Y. H. Ma, "Adsorption and Diffusion of C6 and C8 Hydrocarbons in Silicalite," *Zeolite*, **3**, 118 (1983)

Appendices

1. Experimental Apparatus Set up

The key instrument of this project, the microelectronic recording balance system, has been just set up as shown in *Figure 14*. The gases are introduced into the system at the bottom of the reactor tube of the balance and flow through the adsorbents which are put on the sample pan. The flow rate and fractions of the gases entering the system can be easily controlled by the mass flow controller. One tubular furnace is used to heat the sample zone. The maximum temperature the furnace can reach is 850 °C which is high enough for this project. The pressure or vacuum of the system are detected by the pressure or vacuum sensor. All the parameters such as pressure, temperature, flow rate of gases and weight change of sample with time are recorded in the computer (DTK 486 with notebook software for data acquisition).

The performance of the balance was checked by measuring the adsorption isotherm of hexane (C_6H_{14}) on silicalite with the static equilibrium method. As shown in the *Figure 14*, about 168.8 mg of silicalite pellet was put in the sample pan. The adsorbent was first degassed at 0.1 torr and 350 °C over night (about 20 hours) to remove adsorbed molecules in the adsorbent, followed by cooling to room temperature (about 25 °C). The adsorbate (hexane) was then introduced by evaporating liquid hexane to the system. The uptake curve (weight change of silicalite with time) was recorded in the computer and saved in a data file when the equilibrium was established. The final weight gain was the adsorbed amount of hexane corresponding to the gas pressure in the system. Another uptake curve was then measured by introducing more hexane to a higher pressure. This procedure was repeated till desired final equilibrium pressure was obtained. The adsorption isotherm obtained in our lab, as shown in *Figure 15*, is consistent with the reported data of same system which were also measured by Cahn balance [58]. The adsorption capacity of n-hexane on silicalite obtained in our lab is 1.12

mmole/g, about 20 % smaller than the value reported in the literature (1.42 mmole/g). Since the adsorbent used in this work is pellet which contains some inert binder, while the silicalite used in the literature was powder, a smaller adsorption capacity on silicalite pellet was expected.

Since sulfur dioxide is a very reactive gas, it was not surprised to find that the sulfur dioxide had some detrimental effects on the balance. Because of this, it was difficult to establish a stable state or flat baseline when SO_2 was present in the balance system especially at high SO_2 concentrations. The effects of SO_2 on the weight signal of the balance were tested in several ways. The results are summarized in *Figure 16* and explained below :

- (1). In the first test [*Figure 16 (A)*], no sample was put in the sample pan (quartz). The system was first evacuated to 0.3 torr. The balance was zeroed and a stable base line was obtained in 15 minutes. SO_2 was then introduced to the hangdown tube and was kept in the system. The weight change or weight gain of the sample pan was recorded by the computer. The weight signal increased approximately linearly with time as shown in *Figure 16 (A)*. About 0.05 mg/min drift of the base line was detected at pressure of 1.45 psia. Flat baseline could not be obtained in the recording period (about 40 hours).
- (2). In the second test [*Figure 16 (B)*], the hangdown assembly and extension wire were removed from the balance. Only balance beam was kept in the balance system. The same test as described above was repeated. The weight signal changes with time were recorded as shown in *Figure 16 (B)*. About 0.02 mg/min base line drift was measured. A flat baseline could be established after about 24 hours.
- (3). The result presented in *Figure 16 (C)* is the typical adsorption uptake of SO_2 on our samples. The hangdown assembly, extension wire (about 45 cm), sample pan and sample (DAY zeolite in this test) were put in the balance in this test. The sample were degassed at 350°C and 0.1 torr for 20 hours, followed by cooling to the room temperature. After flat baseline of the balance was established in about 30 minutes, SO_2

was introduced to the balance and kept at the system. The weight changes of the sample with time, as shown in *Figure 16 (C)*, were recorded by a computer. The weight of the sample increased sharply after introduction of SO_2 due to the adsorption of SO_2 by the sample. However, the weight signal would not reach a steady value as long as SO_2 was present in the balance system.

The baseline drift of the balance weight signal made it very difficult to handle sulfur dioxide in the balance. To eliminate or reduce these detrimental effects, the nitrogen purge and baseline correction methods were employed in this work. In the nitrogen purge method, a stream of nitrogen was introduced to the balance system from the vacuum take-out, as shown in *Figure 17*, to protect the beam and circuit of the balance and therefore to reduce the baseline drift.

The high temperature tubular reactor was set up for the chemical and hydrothermal stability test. As shown in *Figure 17*, this apparatus consists of mass flow controllers, a water bubbler, a quartz tubular reactor, and a tubular furnace. The highest temperature the furnace can reach is 1200°C . It is very easy to control the flow rate and concentration of the gas mixture flowing through the samples. The ordinary high temperature furnace can not be used in this study because of the involvement of sulfur dioxide and sulfuric acid.

Schematic Chart of Adsorbent Preparation Procedures

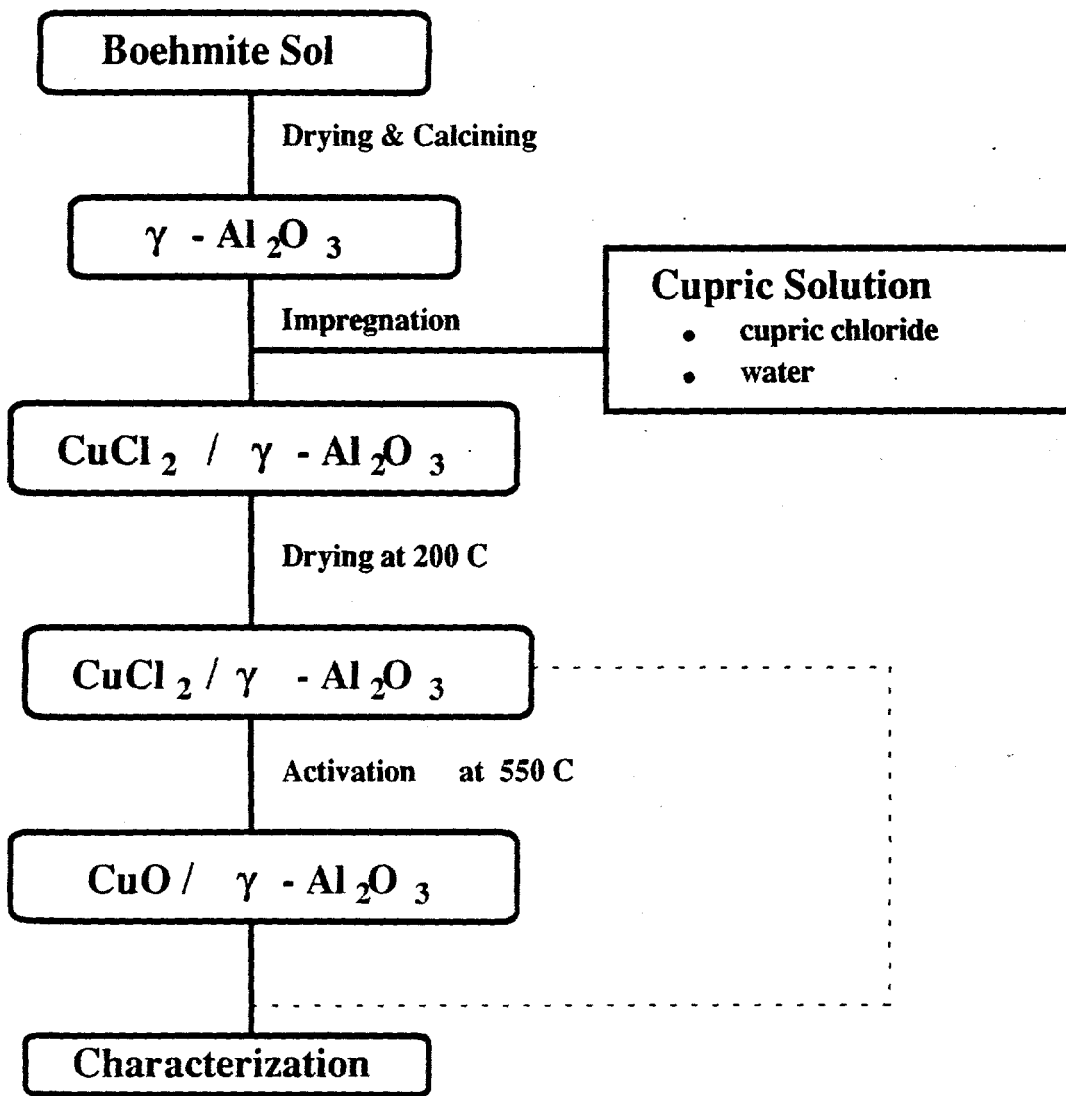


Figure 1

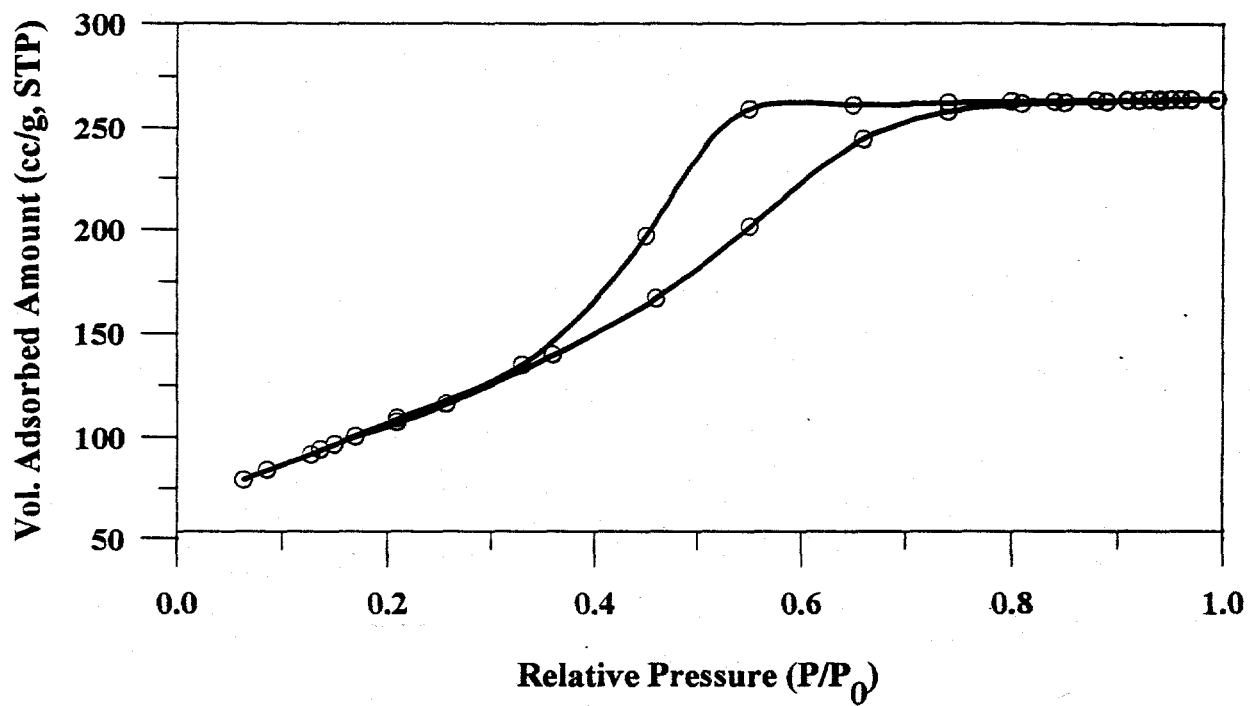


Figure 2. Nitrogen Adsorption/Desorption Isotherm on Copper-1

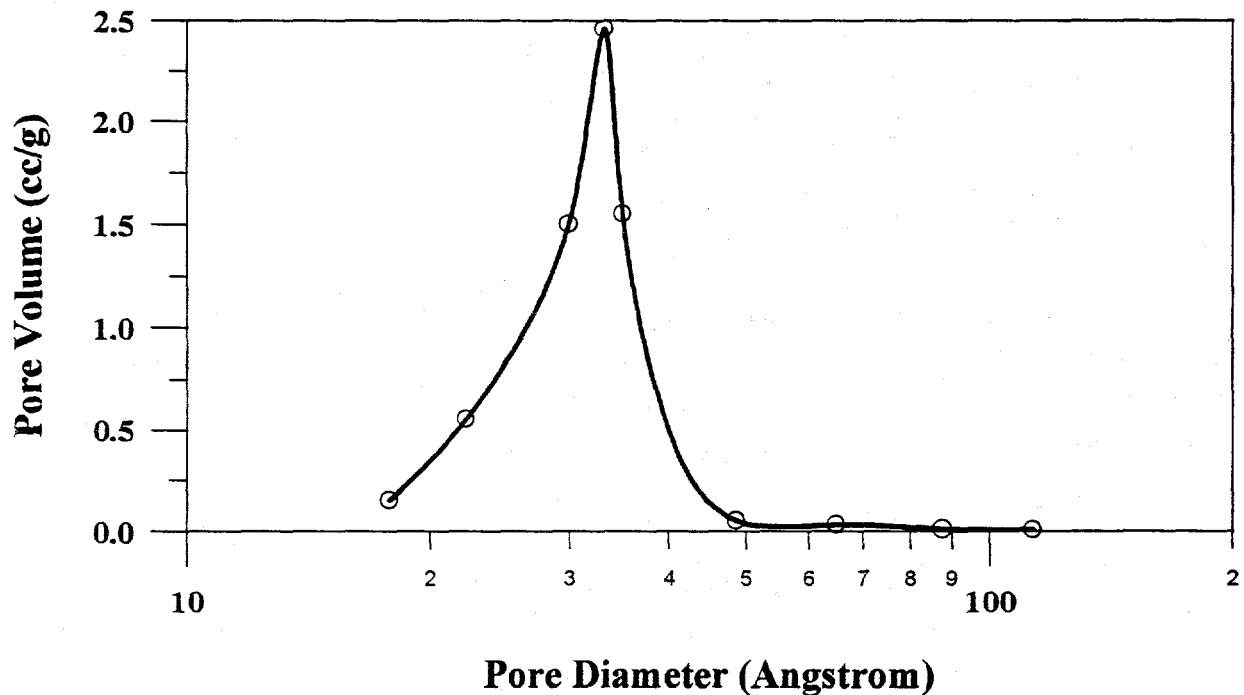


Figure 3. Pore Size Distribution of Calcium-1

XRD Patterns for CuO Sorbents (A) and CaO Sorbents (B)

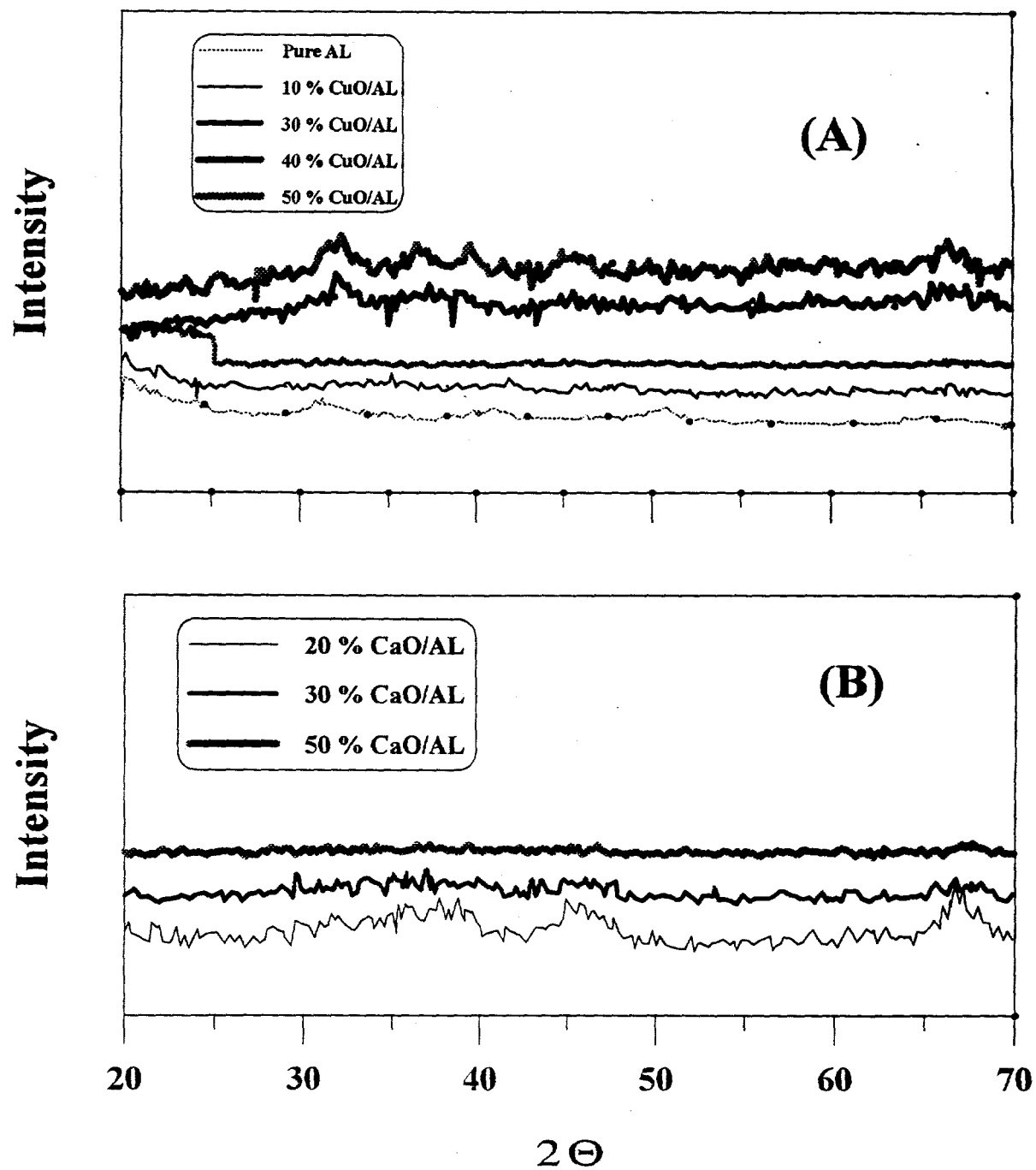


Figure 4

Figure 5. XRD Patterns for Silicalites

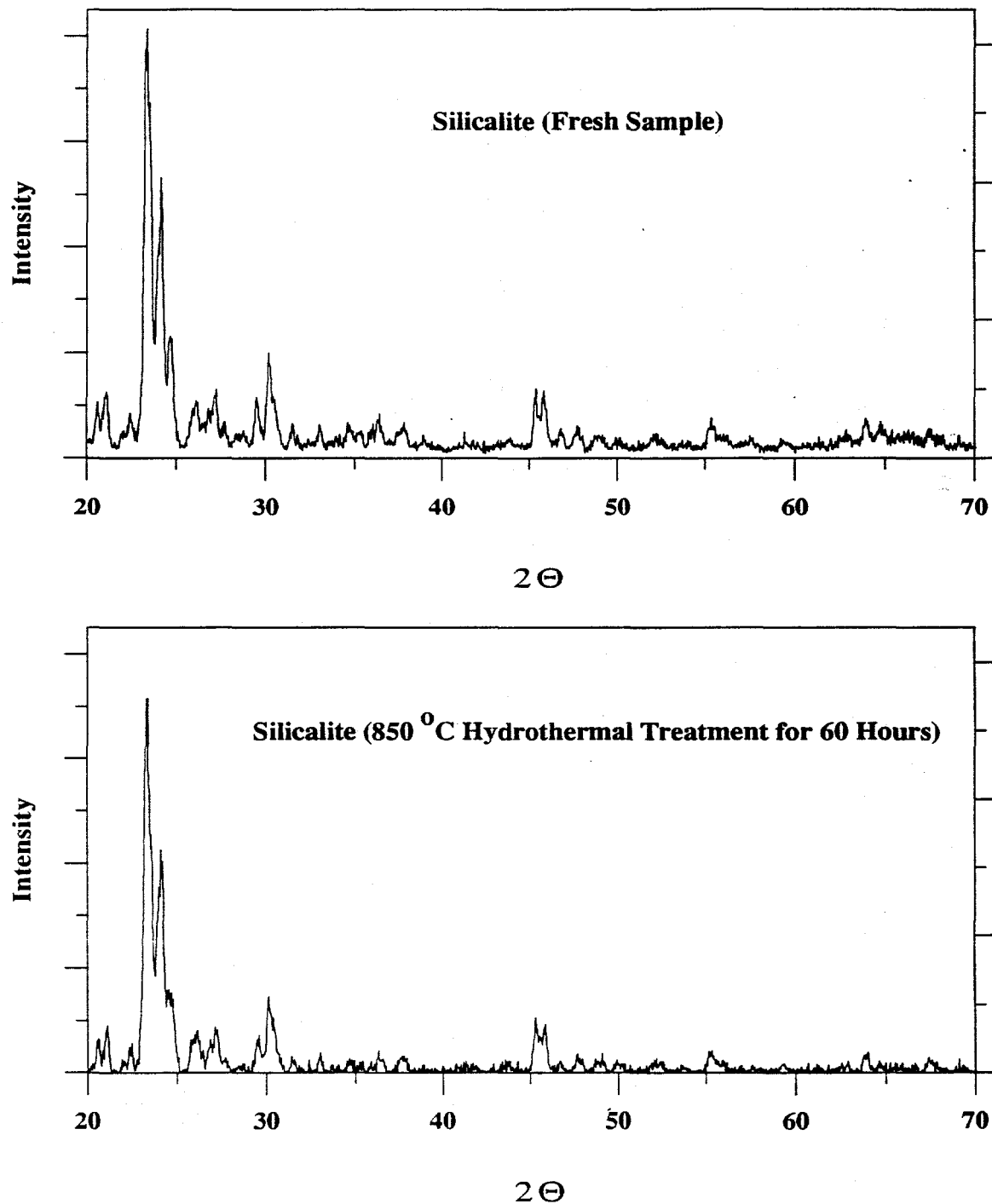
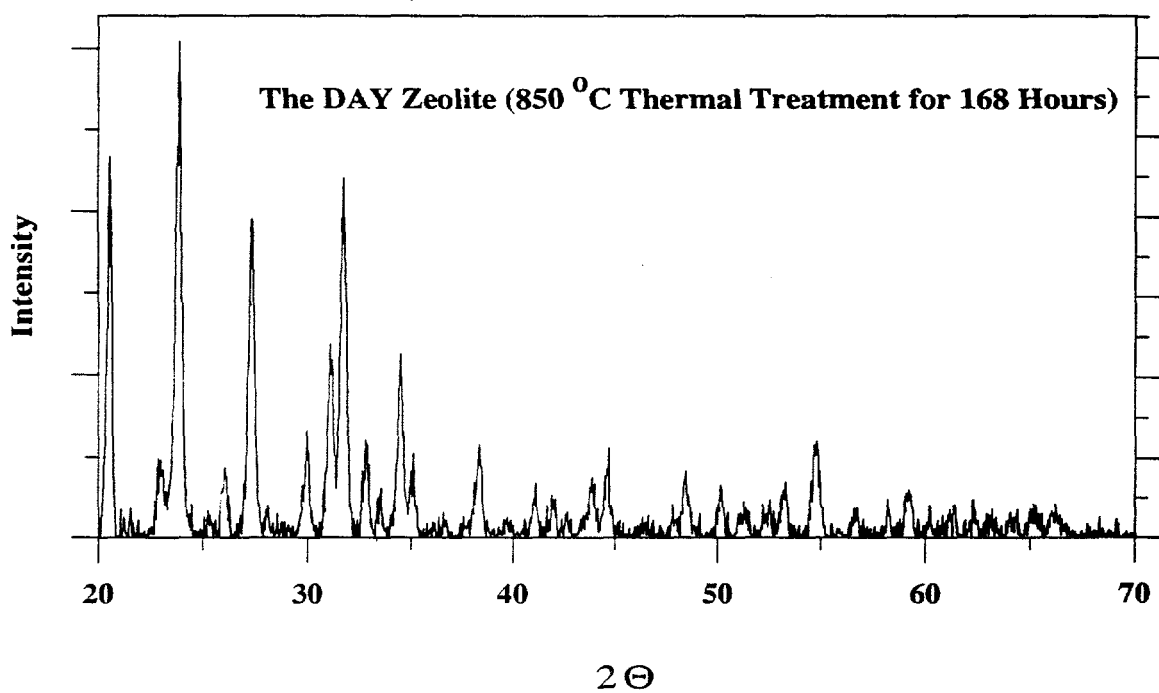
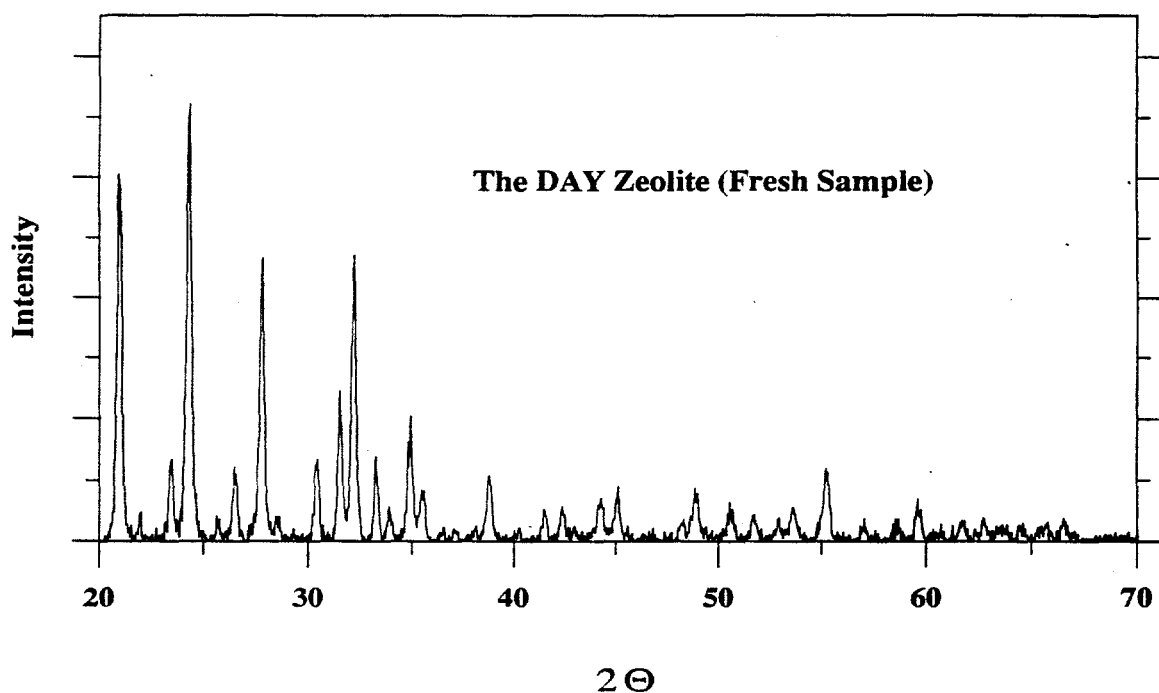
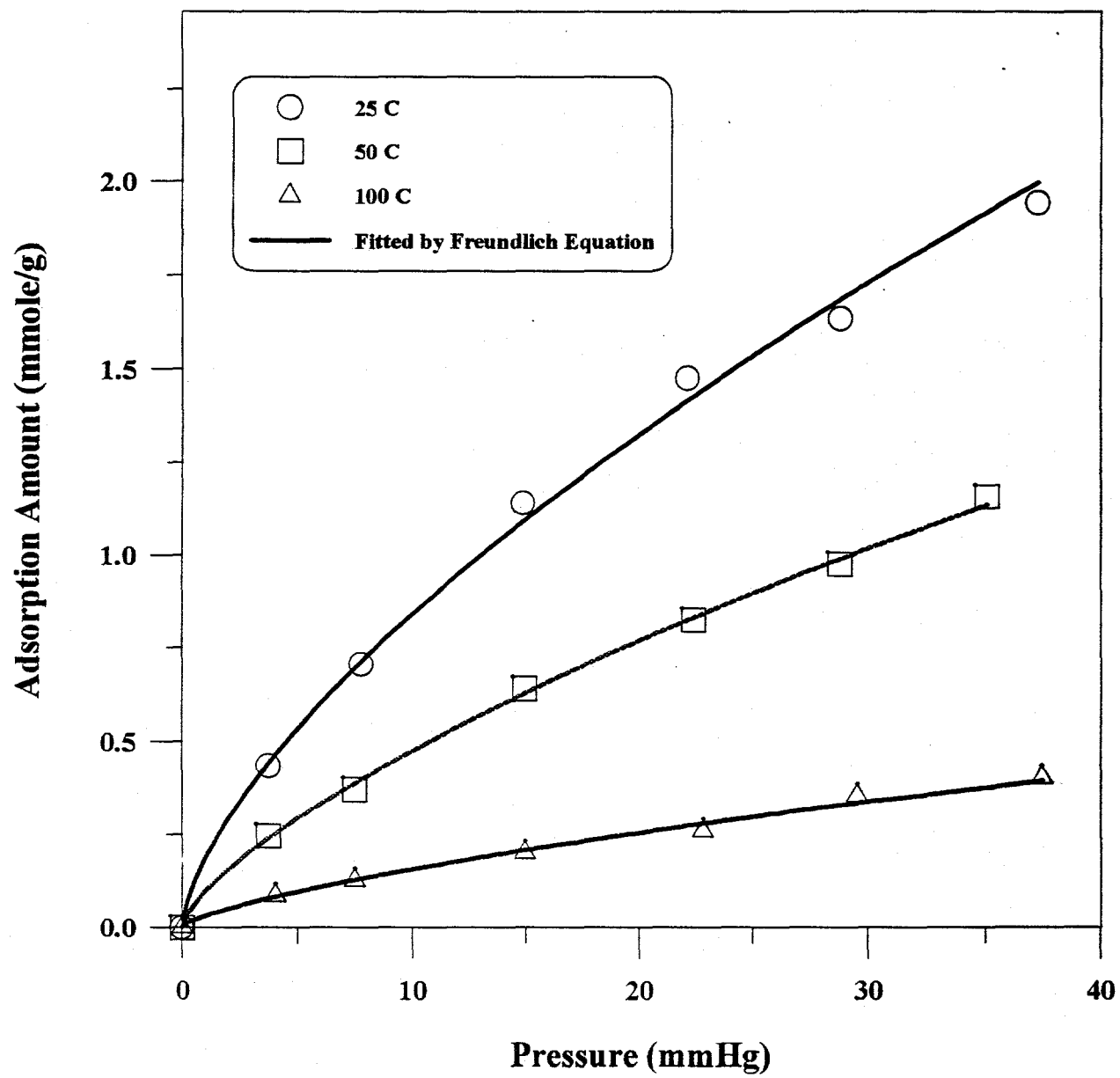


Figure 6. XRD Patterns for the DAY Zeolites



Adsorption Isotherm of SO_2 on Silicalite



Adsorption Isotherm of SO_2 on the DAY Zeolite

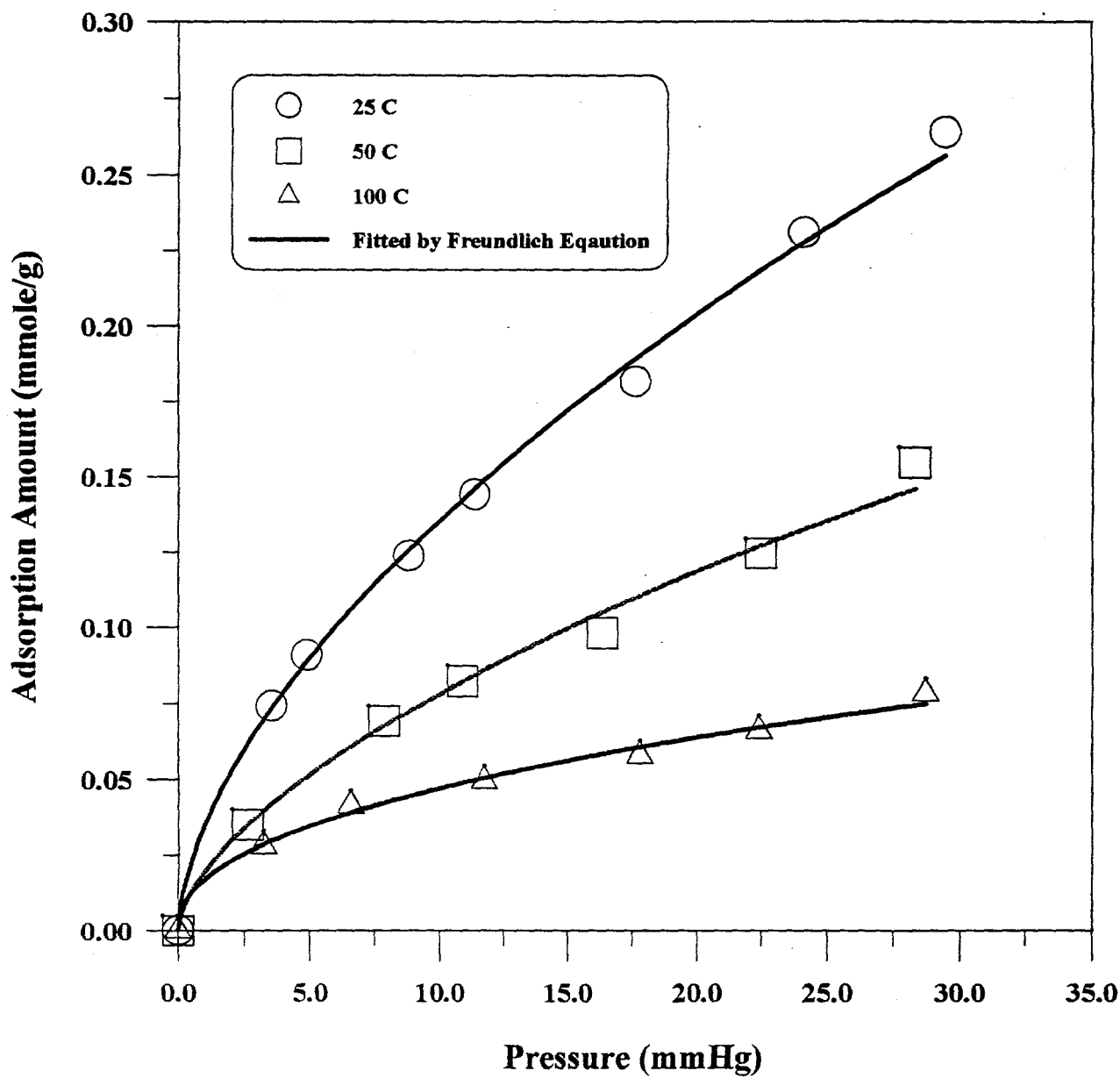


Figure 8

Sulphation Uptake on Copper-4 at 550 $^{\circ}\text{C}$

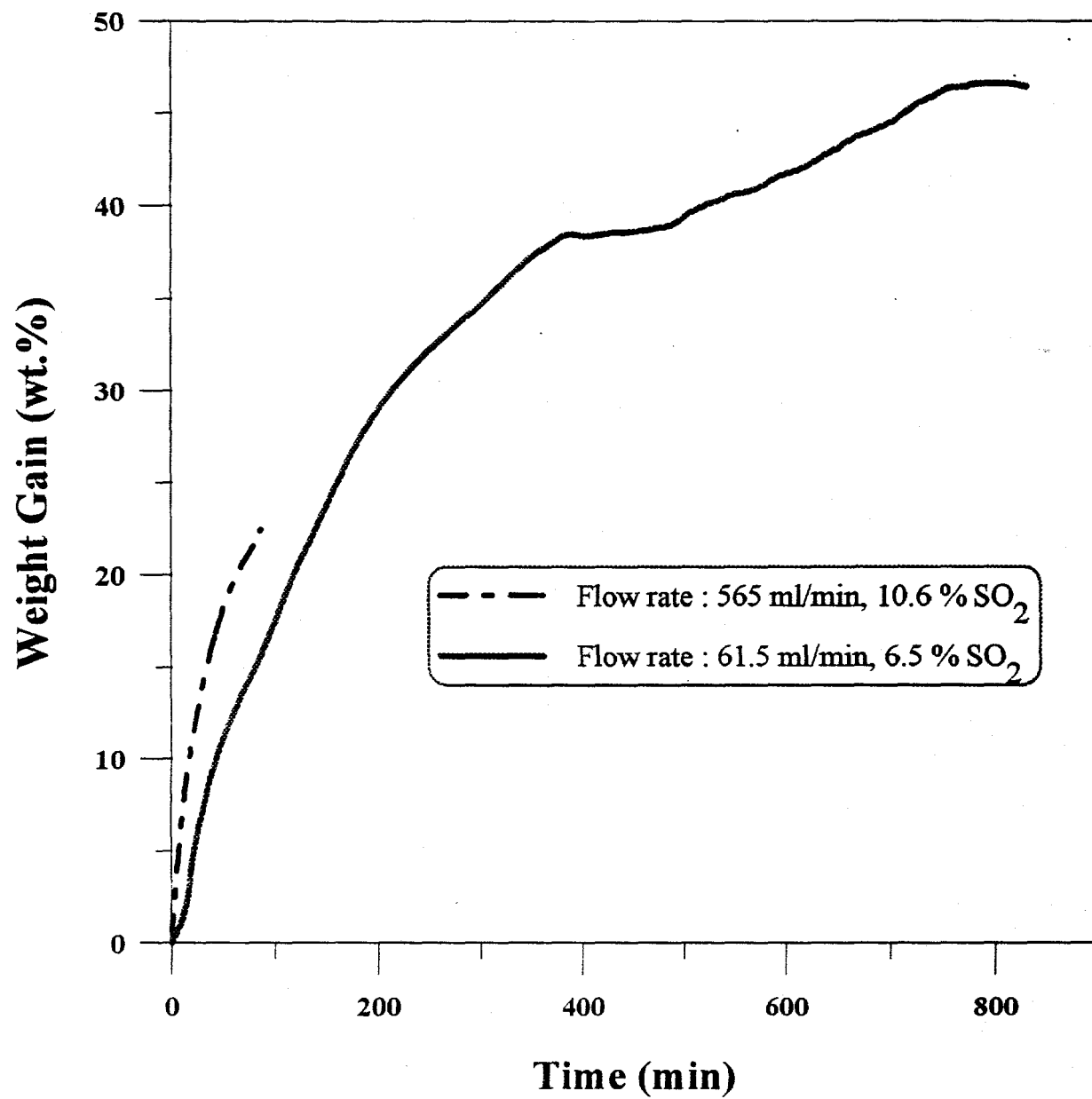


Figure 9

Sulphation Uptake on Calcium-3 at 850 $^{\circ}\text{C}$

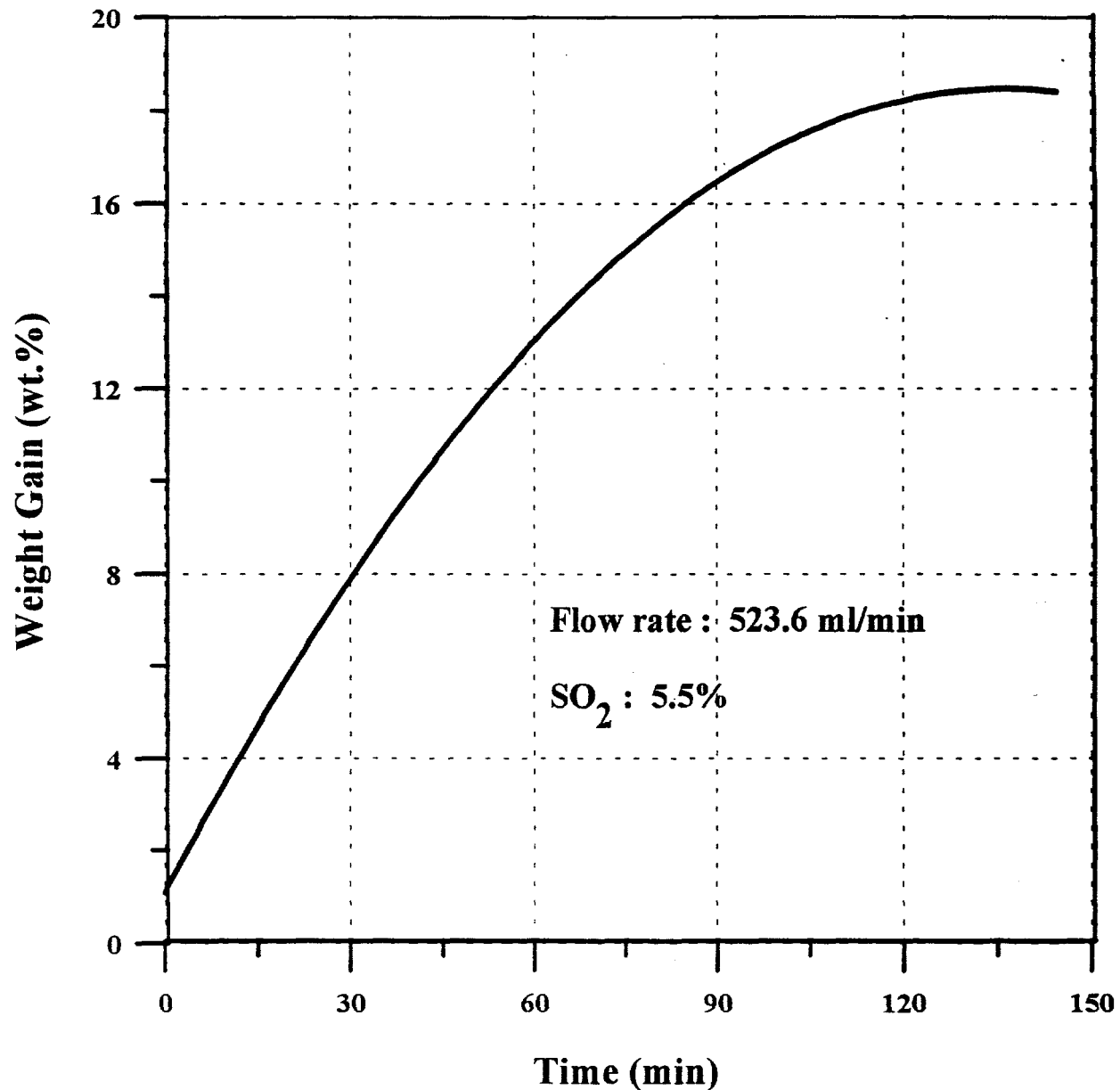


Figure 10

Regeneration Curve on Sulphated Copper-4 at 550 $^{\circ}\text{C}$

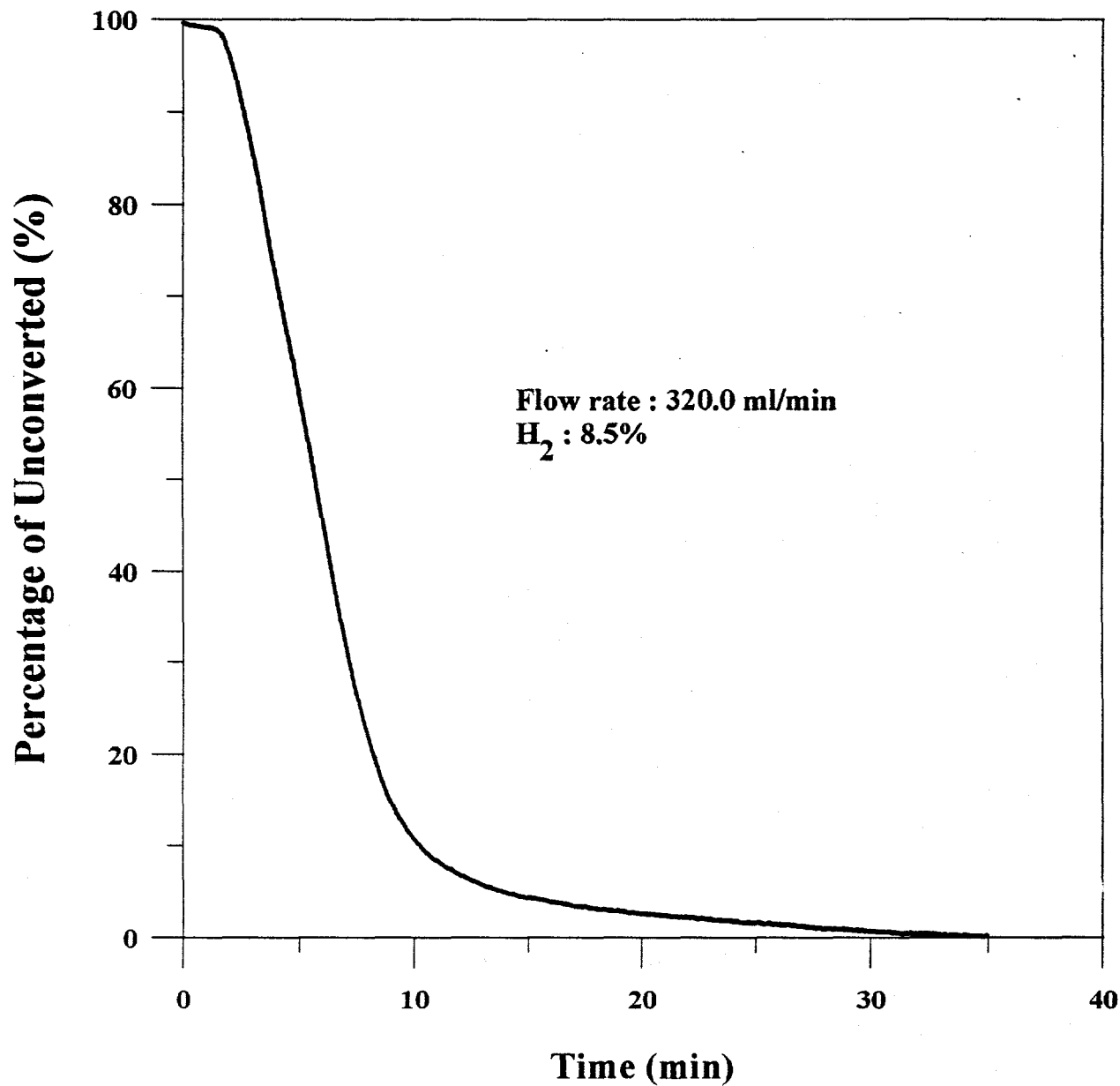


Figure 11

Regeneration Curve of Sulphated Calcium-3 at 850⁰C

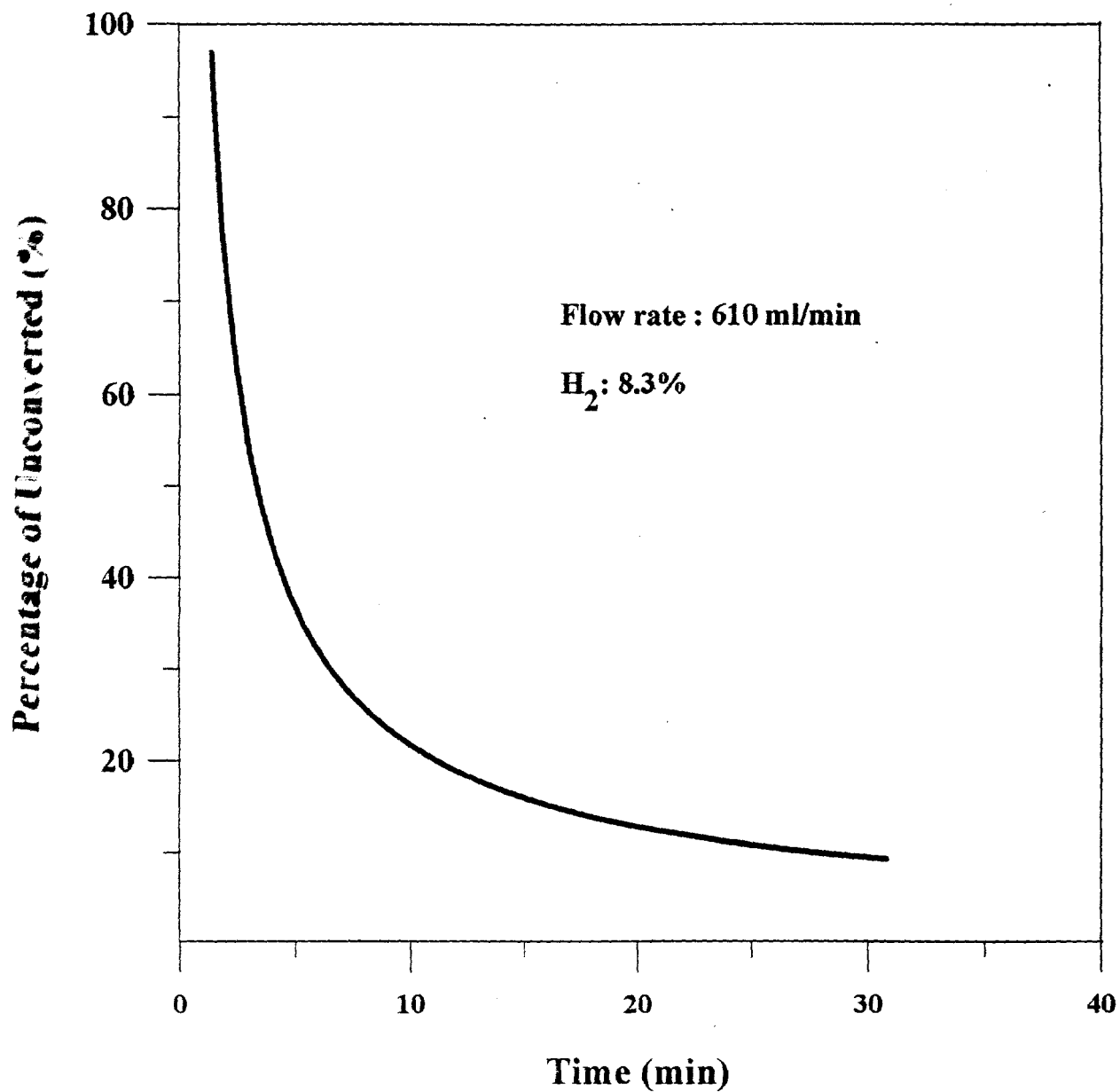
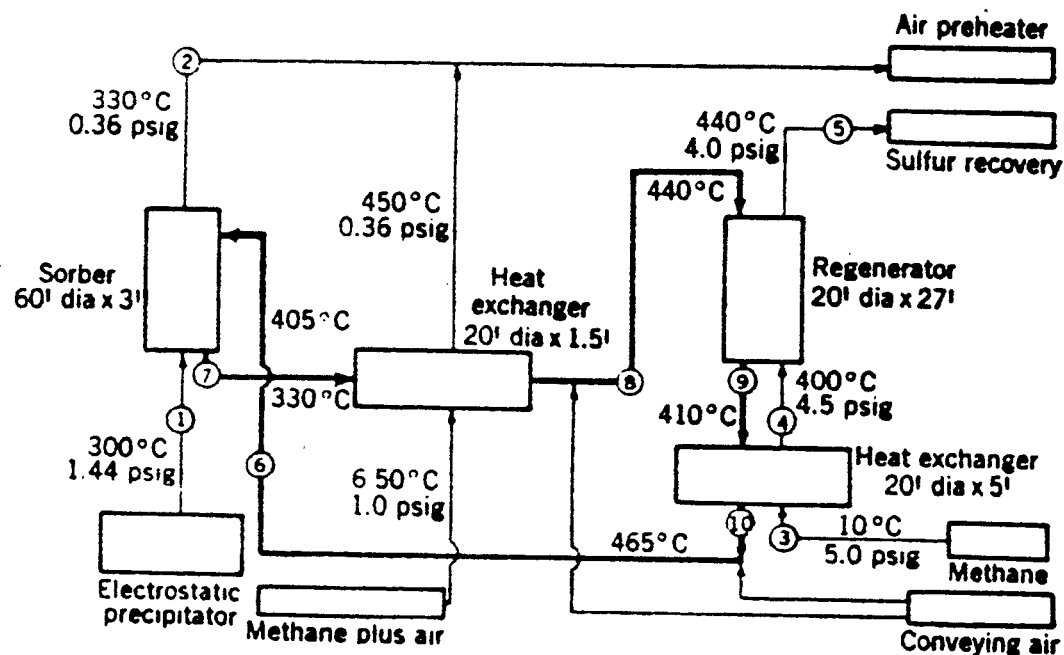


Figure 12



Vessels sized to treat flue gas from 250 MW plant burning 3% sulfur coal.
Vessel heights denote sorbent depth rather than overall height.

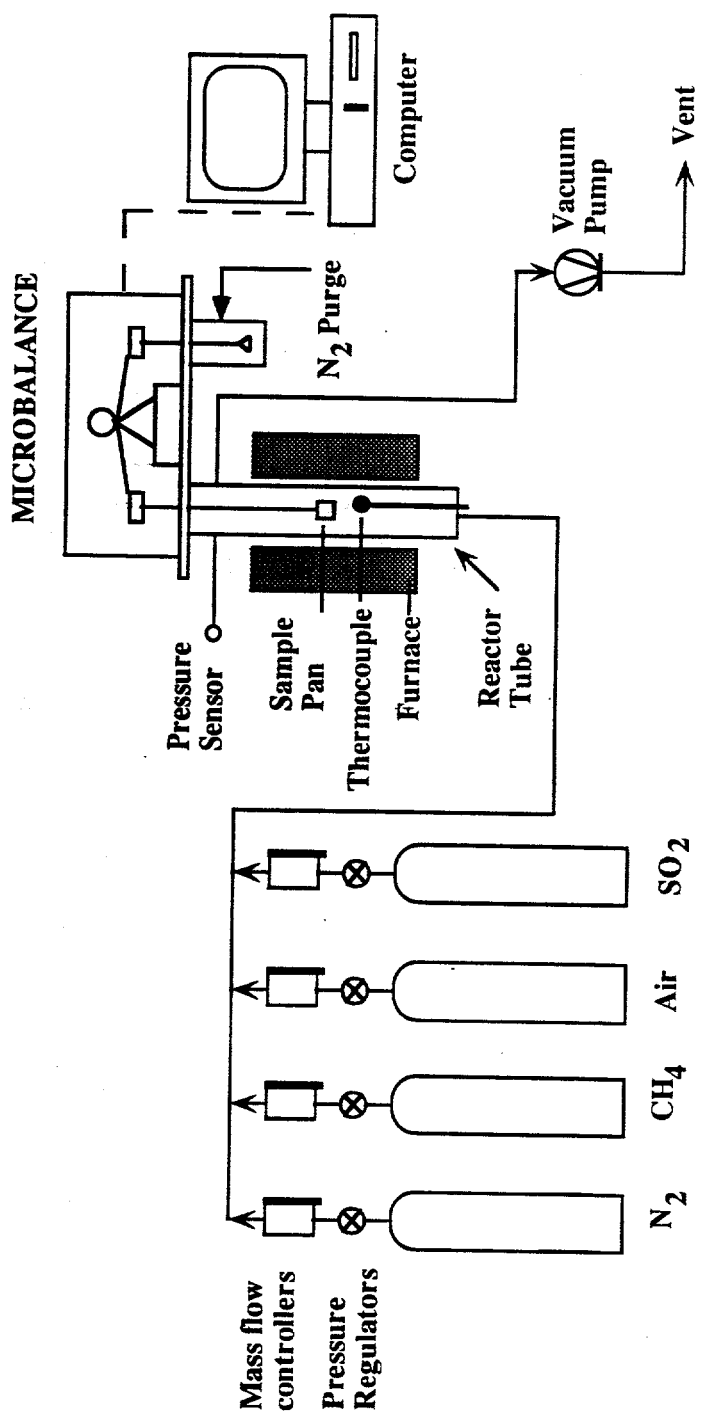
Vessel heights denote sorbent depth rather than overall height. Compositions and rates of numbered streams are given in Table I.

Compositions and rates of numbered streams are shown in table I.

Conceptual Process Flow Sheet for Removal of SO₂ with Copper Oxide

Figure 13

Figure 14



Schematic Diagram of the Electronic Microbalance System
for Adsorption and Desorption Studies

Adsorption Isotherm of Hexane on Silicalite

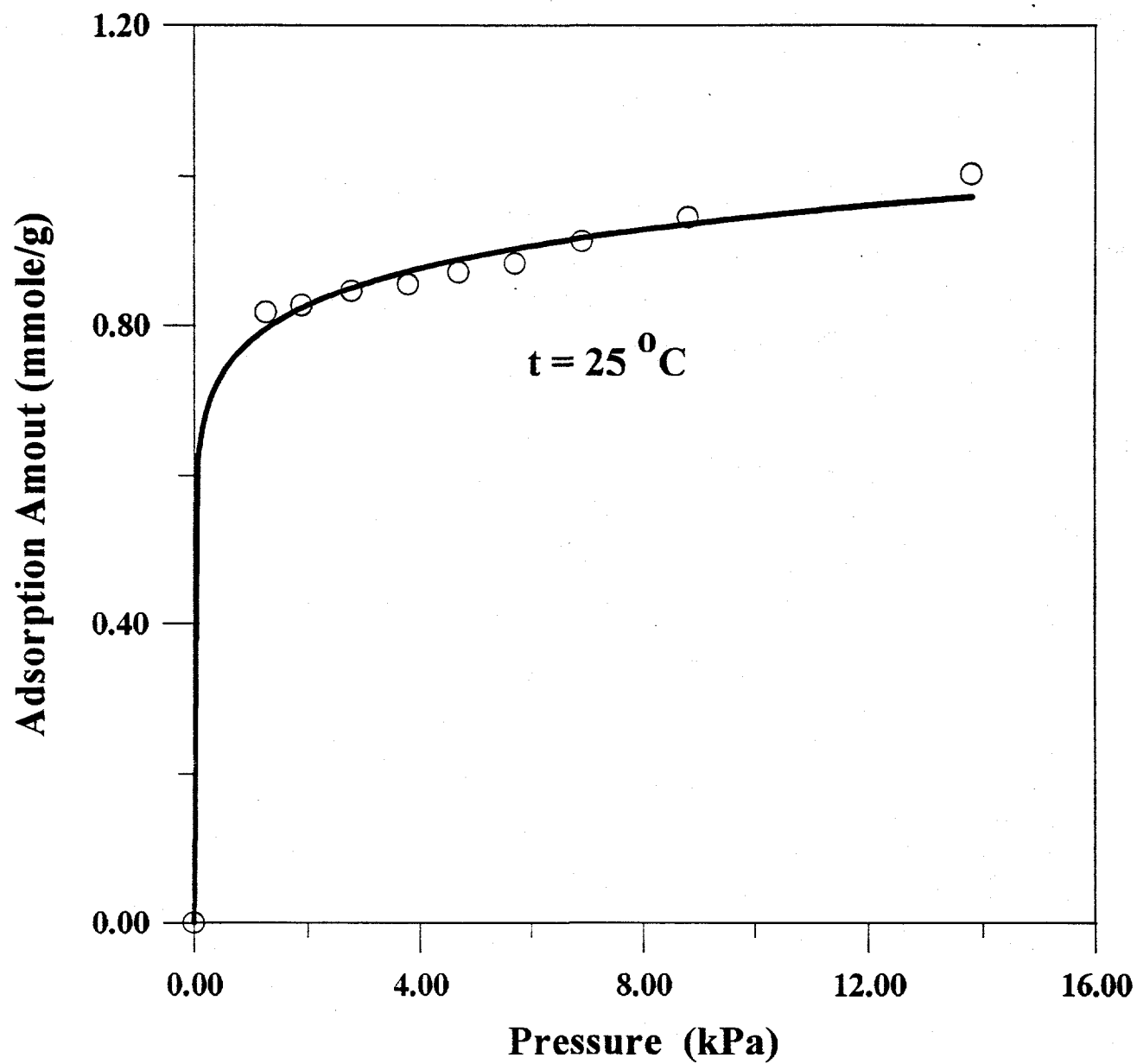
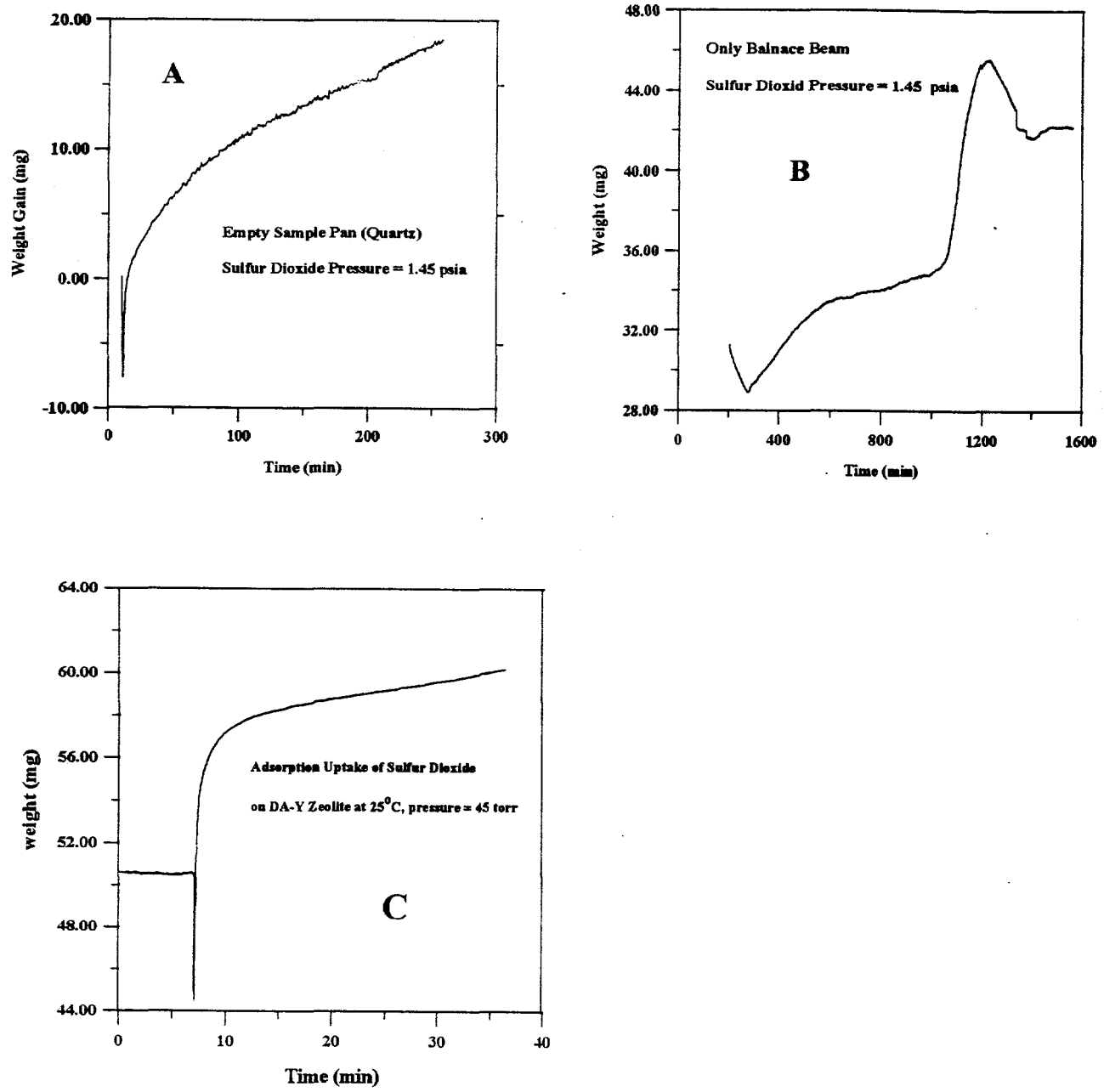


Figure 10



Detimental Effects of Sulfur Dioxide on the Balance

Figure 16

Schematic Diagram of High Temperature Reactor

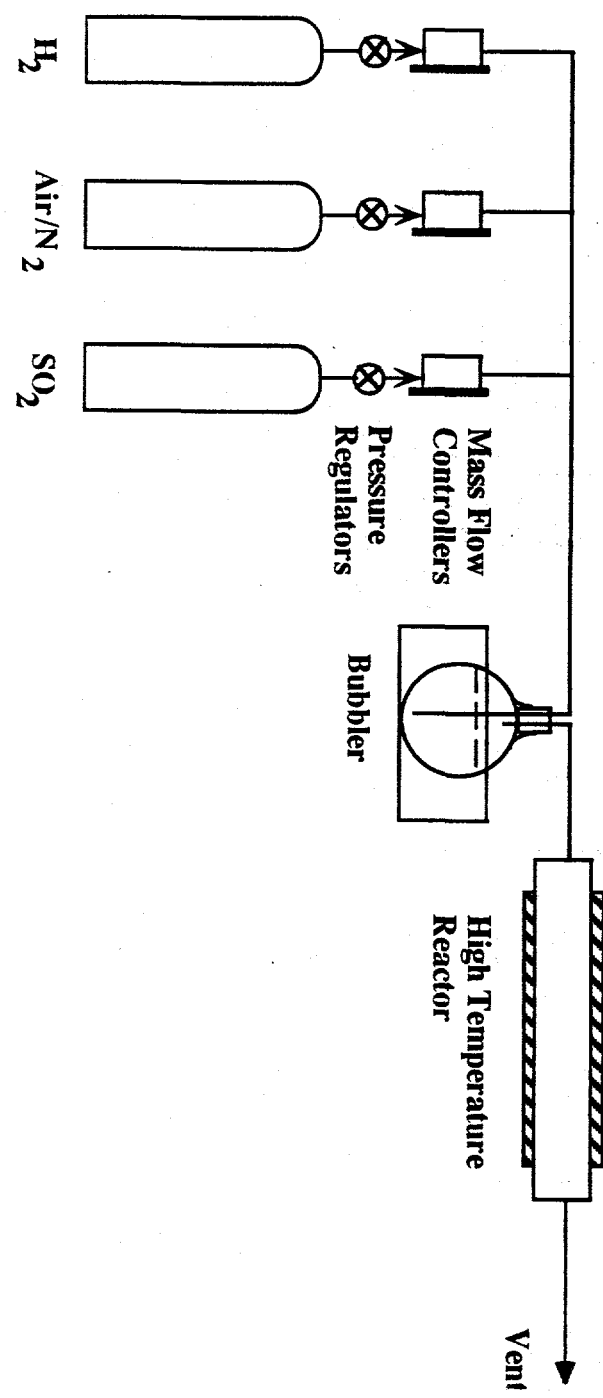


Figure 17

3. Tables in This Report

Table 1. Alumina Adsorbents Prepared by Sol-Gel Technique

Sample No.	Samples	Active Species	Preparation Method
1	alumina	N/A	sol-gel
2	copper-1	CuCl_2	wet-impregnation
3	copper-2	$\text{Cu}(\text{NO}_3)_2$	wet-impregnation
4	calcium-1	CaCl_2	wet-impregnation
5	calcium-2	CaCl_2	sol-solution

Table 2. Pore Texture Data of FGD Adsorbents After Treatment at 550 °C for 6 Hours

Adsorbent Samples	Color	BET Surface Area (m^2/g)	Average Pore Diameter (\AA)	Pore Size Range (\AA)	Pore Volume (cm^3/g)
Alumina#	translucent	304.1	34.6	20~50	0.3866
copper-1	black/green	246.7	42.9	20~60	0.400
copper-2	black/green	235.9	40.8	20~60	0.370
calcium-1	translucent	258.4	35.3	20~60	0.359
calcium-2	white	74.73	35.0	20~50	0.1035

Table 3. Pore Structure Data of CuCl, CuCl₂, and CaCl₂ Coated Alumina Adsorbents with Different Amount of Loading of Active Species

Label of Samples	Coating Precursor	Coating Amount (wt. %)	BET Surface Area (m ² /g of adsorbent)	Corrected BET Surface Area (m ² /g of pure alumina)	Average Pore Diameter (Å)	Pore Volume (cm ³ /g)
Pure Alumina	N/A	N/A	304.1	304.1	34.61	0.399
Copper-3	CuCl	20	328.7	394.4	32.09	0.384
Copper-4	CuCl	30	312.9	406.8	31.69	0.346
Copper-5	CuCl	40	302.2	423.1	31.57	0.332
Copper-6	CuCl	50	273.3	410.0	31.91	0.325
Copper-7	CuCl ₂	29.6	242.1	313.8	33.06	0.299
Copper-8	CuCl ₂	41.9	234.9	333.3	33.09	0.296
Copper-9	CuCl ₂	52.8	221.1	337.8	32.94	0.281
Copper-10	CuCl ₂	62.7	196.6	319.9	33.33	0.256
Calcium-3	CaCl ₂	32.9	237.6	315.7	32.06	0.297
Calcium-4	CaCl ₂	45.7	192.7	280.8	32.34	0.265
Calcium-5	CaCl ₂	66.3	134.7	224.1	33.03	0.183

Table 4. Pore Structure Data of CuO and CaO Alumina
Adsorbents with Different Amount of Loading of Active Species

Label of Samples	Active Species	Loading Amount (wt. %)	BET Surface Area (m ² /g of adsorbent)	Average Pore Diameter (Å)	Pore Volume (cm ³ /g)
Copper-3	CuO	16	261.5	36.0	0.374
Copper-4	CuO	24	257.0	37.4	0.372
Copper-5	CuO	32	240.0	39.8	0.358
Copper-6	CuO	40	211.8	41.3	0.339
Copper-7	CuO	20	214.2	41.8	0.338
Copper-8	CuO	30	186.4	44.9	0.330
Copper-9	CuO	40	107.1	56.6	0.229
Copper-10	CuO	50	115.0	58.3	0.251
Calcium-3	CaO	20	228.26	32.5	0.286
Calcium-4	CaO	30	182.2	32.4	0.233
Calcium-5	CaO	50	249.9	33.6	0.325

Table 5. Pore Texture Data of FGD Adsorbents After 850 °C Treatment for 168 Hours

Adsorbent Samples	Color	BET Surface Area (m ² /g)	Average Pore Diameter (Å)	Pore Size Range (Å)	Pore Volume (cm ³ /g)
copper-1	black/green	107.9	69.98	30~110	.3036
copper-2	black/green	91.4	75.9	30~110	.2687
calcium-1	translucent	109.3	66.09	25~110	.2655
calcium-2	white	55.8	62.47	30~160	.1445

Table 6. Pore Texture Data of FGD Adsorbents after Sulphation at 850 °C for 60 Hours

Adsorbent Samples	Color	BET Surface Area (m ² /g)	Average Pore Diameter (Å)	Pore Size Range (Å)	Pore Volume (cm ³ /g)
Alumina	translucent	185.4	57.1	30~90	0.405
Copper-1	green	83.0	153.6	60~250	0.377
Copper-2	green	67.7	182.4	60~240	0.329
Copper-3	green	86.2	132.8	60~250	0.366
Copper-7	green	78.4	127.6	20~300	0.278
calcium-1	white	86.7	90.8	30~150	0.258
calcium-2	white	57.7	71.5	40~200	0.161
calcium-3	white	95.4	82.7	30~150	0.286

Table 7. Pore Texture Data of the Same Samples Listed in Table 6
after additional 4 Cycles of Sulphation-Reduction-Oxidation

Adsorbent Samples	Color	BET Surface Area (m ² /g)	Average Pore Diameter (Å)	Pore Size Range (Å)	Pore Volume (cm ³ /g)
Alumina	translucent	173.8	60.8	35~110	0.439
Copper-1	black/green	83.9	163.6	60~240	0.365
Copper-2	black/green	62.0	154.2	70~360	0.278
Copper-3	black/green	69.0	159.2	70~250	0.338
Copper-7	black/green	84.1	142.3	50~400	0.380
calcium-1	white	94.7	100.3	40~170	0.330
calcium-2	white	58.2	81.8	40~200	0.178
calcium-3	white	78.8	100.8	60~180	0.268

Table 8. Pore Structure Data of Adsorbents Listed in Table 7 after
Additional Sulphation Treatment under Humid Atmosphere at 850 °C for 60 Hours

Adsorbent Samples	Color	BET Surface Area (m ² /g)	Average Pore Diameter (Å)	Pore Size Range (Å)	Pore Volume (cm ³ /g)
Alumina	translucent	101.3	112.7	40~180	0.391
Copper-1	dark/green	67.1	164.2	60~300	0.319
Copper-2	dark/green	38.4	184.4	100~400	0.144
Copper-3	dark/green	67.0	191.3	70~280	0.215
Copper-7	dark/green	68.2	150.3	70~220	0.332
calcium-1	white	79.9	164.2	60~200	0.319
calcium-2	white	37.6	81.7	30~180	0.103
calcium-3	white	80.7	112.4	40~180	0.282

Table 9. Pore Texture Data of Silicalite and the DAY Zeolite

Sample	BET (m ² /g)	Ave. Pore Size (Å)	Micropore volume (cm ³ /g)
Fresh Silicalite Powder	417.8	4.6	0.154
Silicalite (550 °C Thermal)	432.8	4.7	0.160
Silicalite (850 °C Thermal)	483.9	4.7	0.180
Silicalite (850 °C Sulphation)	394.9	4.7	0.150
Silicalite (850 °C Hydrothermal)	351.9	4.7	0.145
Fresh DAY Zeolite	712.7	6.6	0.351
DAY (850 °C Thermal)	972.3	6.6	0.390
DAY (850 °C Sulphation)	881.9	6.6	0.366
DAY (850 °C Hydrothermal)	1022.1	6.6	0.407

Table 10. Pore Structure and SO₂ Adsorption
Equilibrium and Rate on the DAY Zeolite and Silicalite

	DAY Zeolite	Silicalite
Pore Structure		
Pore Size (Å)	8	6
Pore Volume (cm ³ /g)	0.30	0.19
BET Surface Area (m ² /g)	800	450
SO ₂ Sorption Amount at 25 mmHg (mmole/g)		
25 °C	0.23	1.56
50 °C	0.13	0.88
100 °C	0.07	0.31
SO ₂ Adsorption Rate Constants k (1/Sec) at SO ₂ Pressure of 3.0 mmHg		
25 °C	7.3x10 ⁻⁵	0.50x10 ⁻⁵
50 °C	1.2x10 ⁻⁴	0.77x10 ⁻⁵
100 °C	2.4x10 ⁻⁴	1.50x10 ⁻⁵

Table 11. Freundlich Equation Constants and Heat of Adsorption

	DAY Zeolite		Silicalite	
Freundlich Constants	n	K	n	K
25 °C	1.70	0.035	1.52	0.185
50 °C	1.66	0.020	1.44	0.096
100 °C	2.26	0.017	1.43	0.031
-ΔH (kJ/mole)	6.9		16.9	

Table 12. Adsorption Amount of SO₂ on Silicalites After Different Treatments

(Concentration of SO₂ is 5%)

Treatments	Fresh Sample	550 °C Thermal (168 hours)	850 °C Hydrothermal (68 hours)	850 °C Thermal (168 hours)
Ads. Amount (mmol/g)	1.94	1.82	1.79	1.65

Table 13. Comparison of Sulphation Uptakes on CuO Adsorbents

	Copper-4	Centi et al. (1992a)
BET Area (m ² /g)	257.0	110.0
CuO Loading	24 %	8.2 %
Temperature (°C)	550	300
SO ₂ % in Gas Stream	6.5%	1400 ppm
Flow Rate (ml/min)	61.5	100
Equilibrium Uptake (wt.%)	45 %	7 %
Equilibrium SO ₂ to CuO Ratio	1.86	0.78
Time for 5 % Uptake (min)	6.5	20

Table 14. Comparison of Regeneration Kinetics on Copper Oxide Adsorbents

	Copper-4	Harriot et al. (1992)
Temperature (°C)	550	450
SO ₂ Uptake (mmole/g)	5.66	1.03
Reducing Gas	18.5 % H ₂ + N ₂	30 % CH ₄ + N ₂
Flow Rate (ml/min)	320	1000
Time for 90% Conversion (min)	10	20

Table 15. Rate and Composition of Major Process Streams for
Removal of SO₂ from 250 Mw Power Plant with Copper Oxide Adsorbent

		Gas Stream							
		1	2	3	4	5			
1b mol/hr	vol %	1b mol/hr	vol %	1b mol/hr	vol %	1b mol/hr	vol %	1b mol/hr	vol %
SO ₂	155	0.215	15.5	0.0215	0	0.0	0	0.0	139
SO ₃	0	0.0	0.0	0.0	0	0.0	0	0.0	38.1
H ₂ S	0	0.0	0.0	0.0	0	0.0	0	0.0	Tr.
Cl ₁₁	0	0.0	0.0	0.0	87.1	100.0	87.1	100.0	17.4
H ₂ O	5880	8.15	5880	8.18	0	0.0	0	0.0	4.76
O ₂	2380	3.30	2310	3.21	0	0.0	0	0.0	139
N ₂	53800	74.5	53800	74.7	0	0.0	0	0.0	38.1
CO ₂	9970	13.8	9970	13.9	0	0.0	0	0.0	0.0
Solid Stream									
		6	7	8	9	10			
1b / hr	g S/100g*	1b / hr	g S/100g	1b / hr	g S/100g	1b / hr	g S/100g	1b / hr	g S/100g
305000	1.0	317000	2.5	317000	2.5	303000	1.0	303000	

* Concentration is given as g sulfur per 100 sulfur-free adsorbent